

Ab initio studies on the photodissociation dynamics of the 1,1-difluoroethyl radical

Journal Article**Author(s):**

Fritsche, Lukas; Bach, Andrea; Chen, Peter

Publication date:

2018-02-28

Permanent link:

<https://doi.org/10.3929/ethz-b-000249991>

Rights / license:

[In Copyright - Non-Commercial Use Permitted](#)

Originally published in:

The Journal of Chemical Physics 148(8), <https://doi.org/10.1063/1.5007152>

Ab initio studies on the photodissociation dynamics of the 1,1-difluoroethyl radical

Lukas Fritsche, Andreas Bach and Peter Chen
Laboratorium für Organische Chemie, ETH Zurich, Wolfgang-Pauli-Strasse 10,
CH-8093 Zürich, Switzerland

BOMD trajectory calculations at the HCTH147/6-31G** level of theory simulate the dissociation dynamics of photolytically excited 1,1-difluoroethyl radicals. EOMCCSD/AUG-cc-pVDZ calculations show that an excitation energy of 94.82 kcal/mol is necessary to initiate photodissociation reactions. In contrast to photodissociation dynamics of ethyl radicals where a large discrepancy between actual dissociation rates and rates predicted by statistical rate theories, we find reaction rates of $5.1 \cdot 10^{11} \text{ s}^{-1}$ for the dissociation of an H atom, which is in perfect accordance to what is predicted by RRKM calculations and there is no indication of any nonstatistical effects. However, our trajectory calculations show a much larger fraction of C-C bond breakage reaction of 56% occurring than expected by RRKM (only 16%).

I. INTRODUCTION

The 1,1-difluoroethyl radical is an interesting model compound for the ethyl radical with two hydrogen atoms substituted by fluorine. Ethyl radicals play an important role in combustion processes and are important intermediates in hydrocarbon crackers. Ethene is formed from ethyl radicals through the loss of a hydrogen atom and features a key role in petrochemical industry. Therefore, the

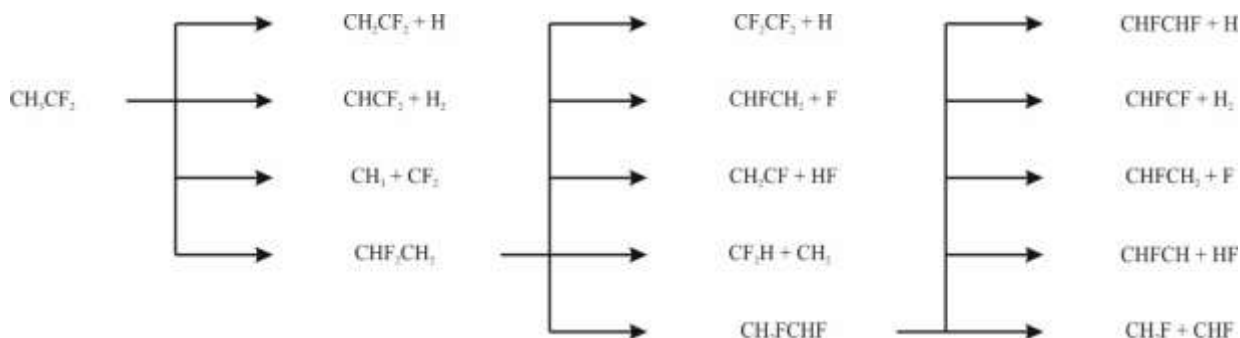


FIG. 1 Dissociation products of the 1,1-difluoroethyl radical. Due to the substitution with fluorine, much more reaction channels exist than for the dissociation of unsubstituted ethyl radicals.

kinetics of this reaction is of high interest and it is not surprising that the dynamics of this reaction has been investigated extensively in photodissociation experiments¹⁻⁷ and in theory⁸⁻¹¹.

Dissociation dynamics of the ethyl radical have been studied by Hase *et al* with chemical dynamics simulations. Although the dynamics of the dissociation reaction have been found to be in accord with the Rice-Ramsperger-Kassel-Marcus (RRKM) theory¹²⁻¹⁵, the classical microcanonical rate constants have been found to be much smaller than predicted by RRKM due to anharmonicity. Inconsistencies between theoretical and experimental thermal kinetics remain for the $\text{H} + \text{C}_2\text{H}_4 \rightleftharpoons \text{C}_2\text{H}_5$ association and dissociation reactions^{16, 17}. Furthermore, recent work in our group simulated the dissociation process with direct dynamics classical trajectory calculations resulting in a number of trajectories with a much longer lifetime than predicted by RRKM^{18, 19}. This leads to the

conclusion that the dissociation of ethyl radicals must possess nonstatistical dynamics.

The intention of this work is thus to compare dissociation reactions of the 1,1-difluoroethyl radical with those occurring from ethyl radicals to explore the impact of substitution with fluorine on the statistical behavior of the decomposition. We explore the dissociation of 1,1-difluoroethyl radical by comparing RRKM kinetics and Born-Oppenheimer Molecular Dynamics (BOMD)

trajectory simulations.

In this work we simulate a photodissociation process, where a photon excites the 1,1-difluoroethyl radical to an excited state, which yields the required reaction energy for the dissociation after internal conversion. Thus, we calculate the excitation energy of 1,1-difluoroethyl radical to this first excited (3s) Rydberg state. Within the RRKM approach we expect that after excitation the dissociations proceed by internal conversion to the ground state. The ground state PES covers the 1,1-difluoroethyl radical plus dissociation products and transition states. In comparison with the ethyl radical, the 1,1-difluoroethyl radical exhibits more decomposition pathways as displayed in Figure 1, including dissociation of fluorine atoms, hydrogen fluoride as well as H shift and F shift reactions.

We intend to take into account all possible reaction channels for a proper investigation of the dissociation of 1,1-difluoroethyl radicals and explore whether the dissociation to other products can compete with the

formation of 1,1-difluoroethene and affect the kinetics of the overall decomposition. Other publications show that there are other important reaction channels in the decomposition of similarly sized hydrocarbon radicals²⁰.

II. COMPUTATIONAL METHODS

We simulate the photodissociation dynamics of the 1,1-difluoroethyl radical two theoretical models, the harmonic Rice-Ramsperger-Kassel-Marcus (RRKM) theory approach based on computationally derived energy surfaces and Born-Oppenheimer Molecular Dynamics (BOMD) trajectory calculations.

For the statistical modeling of photodissociation rates, we use the MultiWell software package²¹⁻²³ that is based on the RRKM model. The software tool DenSum provides exact counts for sums and densities of states using the Stein-Rabinovitch extension²⁴ of the Beyer-Swineheart algorithm²⁵. As a data input, reaction paths need to be defined within the reaction system. The program requires inputs of relative energies of products and activation energies of reaction intermediates (wells). We consider paths leading to a well as reversible and reactions to a dissociation product as irreversible. Barrierless dissociations such as the C-C bond cleavage are treated in a loose transition state model that is employed in the CRUNCH data analysis program²⁶⁻²⁸. Rates of the barrierless dissociations generated by the CRUNCH data analysis program serve as input to the MultiWell program package. We discuss the suitability of this method in the Results part.

To generate the required PES, we optimize all structures using a Hamprecht-Cohen-Tozer-Handy functional²⁹ with a relatively small basis set (HCTH147/6-31G**). Density functional theory (DFT) calculations are performed with GAUSSIAN 09³⁰. This method should be sufficient for an accurate structure determination. Previous work on the ethyl radical³¹ shows that this functional reproduces energies obtained using CCSD(T) extrapolated to the complete basis set (CBS) limit, exceptionally well. In addition, the structures of some key components are optimized by the more accurate CCSD(T)/cc-pVTZ³² level of theory and show a very small deviation in terms of atomic coordinates compared to the DFT-optimized structures (see appendix). Single point calculations at the CCSD(T)/cc-pVTZ level of theory refine the energy levels of all structures in the reaction system. We use both, the GAUSSIAN 09 and the CFOUR program package³³ to perform calculations at the coupled cluster level of theory. There are no differences in energies that can be assigned to the choice of the program package. Single point energies of all structures occurring in the most probable reaction channels are determined using CCSD(T)/cc-pVTZ-F12 calculations and the resulting relative energies for the relevant reaction channels are compared to the ones obtained using the smaller cc-pVTZ basis set in the coupled cluster methods. The UCCSD(T)/cc-pVTZ-F12 is implemented in the MOLPRO³⁴⁻³⁶ program package and is considered to yield reliable estimations of energies at the (CBS) limit.

We use the HCTH147/6-31G** method for a frequency analysis to derive the vibrational frequencies for the zero-potential-energy (ZPE) corrections. To determine the excitation energy of 94.8 kcal/mol, we optimize the structure of the 1,1-difluoroethyl radical in the first excited state using the equation of motion coupled cluster theory with singles and doubles excitations with an augmented correlation consistent double zeta valence basis set (EOM-CCSD/AUG-cc-pVDZ).

In a Born-Oppenheimer molecular dynamics approach at the HCTH147/6-31G** level of theory we simulate 500 trajectories of the 1,1-difluoroethyl radical. We generate a microcanonical ensemble which is excited by the same excitation energy that is used in the RRKM approach and read in the resulting initial Cartesian coordinates and velocities externally using quasiclassical normal mode sampling¹⁸. The maximum number of steps for the BOMD trajectories is 20'000. An interfragment gradient of $3 \cdot 10^{-5}$ to $3 \cdot 10^{-7}$ serves as additional stop criterium. We evaluate trajectories manually and assign each of them to a certain reaction path. A FORTRAN program integrates the state probabilities in time steps of 0.1 ps.

Regarding the computational costs for the BOMD trajectory calculation, we are bound to the more resource efficient DFT-methods instead of an ab initio approach. Since for similar systems, the HCTH147 functional has been shown to reproduce energies obtained by CCSD(T) extrapolated to the CBS limit very well³¹, it has been used for this study as well. Use of the same functional and basis set for both ways of determining the photodissociation rates allows a good comparability.

III. RESULTS

A. Potential energy surfaces

The high excitation energy of 94.8 kcal/mol used for the simulation of the dissociation dynamics render reaction channels other than the dissociation of a hydrogen atom with a dissociation energy of 39.8 kcal/mol possible. Figures 1-3 give an overview over the possible dissociation channels of 1,1-difluoroethyl radical. The number in brackets is an index for the reactions or rather the reaction products, where the reactant holds number (0). The fluorine substituents largely destabilize the carbon-carbon bond and make the fission of this bond (3) more likely. Furthermore, instead of the loss of a hydrogen atom, the molecule could undergo a 1,2-hydrogen shift.

Other than in the ethyl radical, where such a shift reaction just generates the starting material, in the 1,1-difluoroethyl radical, the product of the shift is not the same as the starting material and opens a large variety of sequential reactions. FIG. 2 shows possible dissociation reactions of the 1,1-difluoroethyl radical after a 1,2-hydrogen shift (5)-(9). Dissociation of H-radical again results in the formation of 1,1-difluoroethene, reaction products (1) and (5) are the same but different starting materials and transition states. In addition to the reaction types that are already discussed in Figure 1, one now has to take into account fluorine radical dissociations (6) and the elimination of hydrogen fluoride (7).

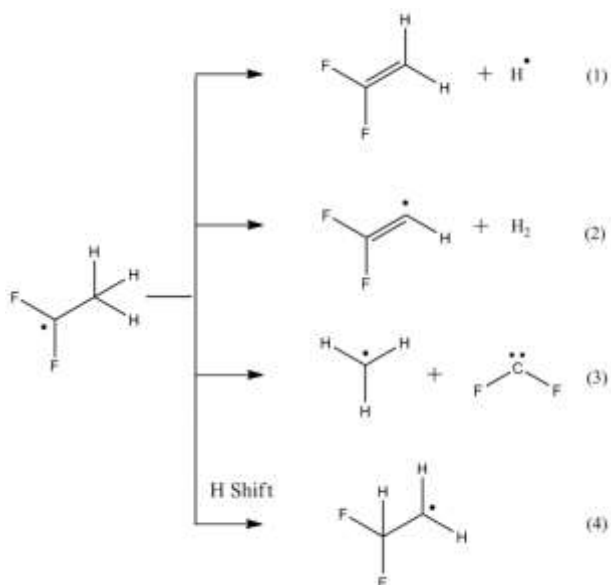


FIG. 2: Reaction channels of the photolytically excited 1,1-difluoroethyl radical including H radical dissociation, H₂ elimination, C-C bond breakage and 1,2-H shift.

Yet another reaction channel opens with the formation of (4), the 1,2-F-shift reaction leading to the formation of 1,2-difluoroethyl radical (9) and thus yet to another bunch of possible reactions, which are drawn in Figure 3 (10)-(17). The types of reactions are the same as already described so far in Figures 1 and 2.

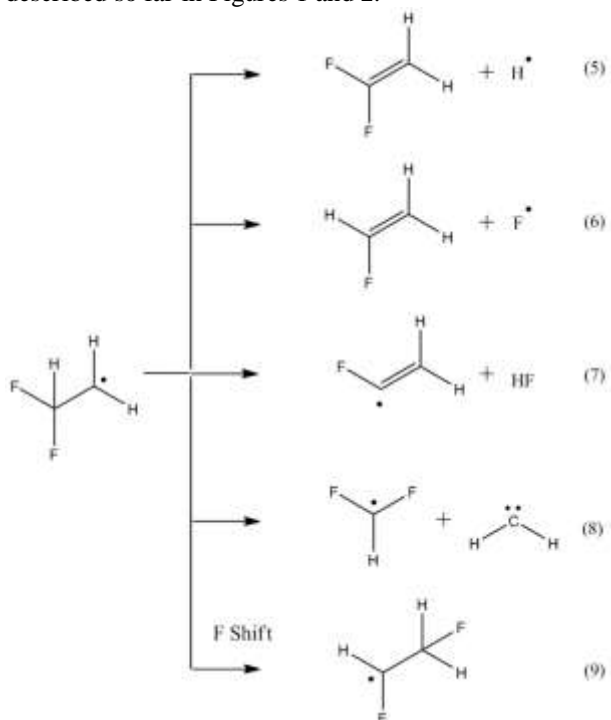


FIG. 3: Reaction channels taken into account from the 1,1-difluoroethyl radical after an H-shift reaction (4). Possible dissociation channels are the loss of a hydrogen radical (5), fluorine radical dissociation (6), elimination of hydrogen fluoride (7), C-C bond fission and 1,2-shifting of a fluorine atom.

Due to a reduction of symmetry during the fluorine shift reaction, several reactions can now lead to multiple isomers such as the H dissociation reaction leading to the formation of either *cis*- or *trans*-1,2-difluoroethene. The reaction

product of the loss of a fluorine atom (14) is the same as reaction product (6) but again with different starting material and transition state.

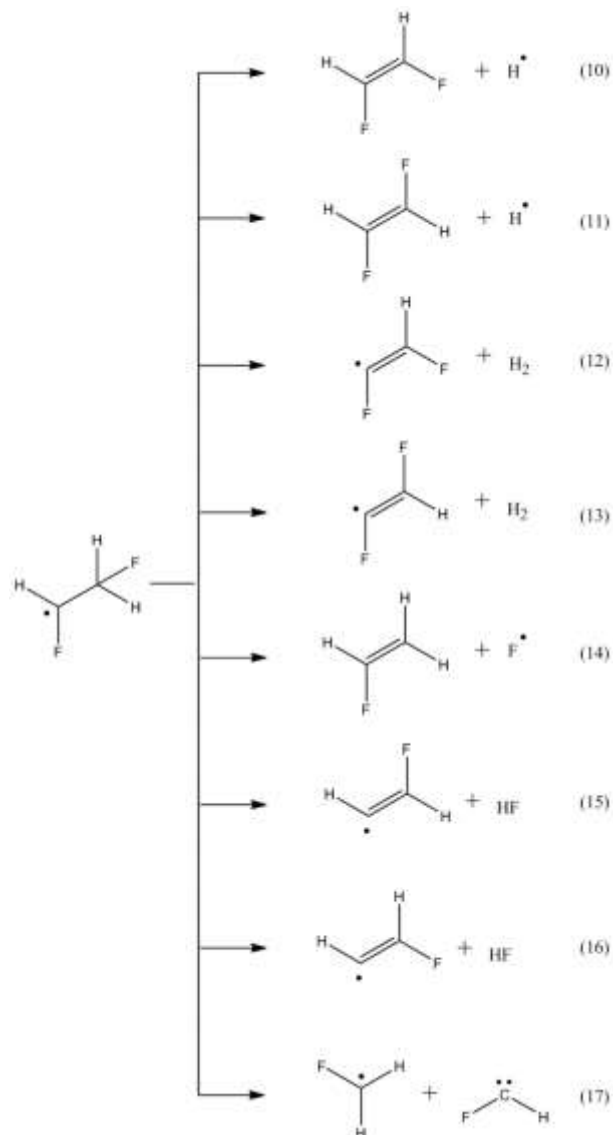


FIG. 4: Reaction channels taken into account outgoing from the 1,2-difluoroethyl radical (9).

For a proper investigation on the dissociation dynamics, we must take into account all the reaction channels. A comparison between the results of both methods gives us hints whether nonstatistical effects can occur in such small molecules and how the dissociation dynamics of the ethyl radical changes due to a substitution with fluorine atoms.

As mentioned above, we model the ground state potential energy surface including many dissociation channels for the 1,1-difluoroethyl radical. Figure 4 shows a simplified overview of the energetic landscape with single point energy levels derived at the CCSD(T)/cc-pVTZ level of theory. The numbers in brackets correspond to the reactions with the same number shown in Figures 1-3. Reaction path (1) leads therefore to product(s) (1) and so on.

Calculated reaction energy results of both levels of theory indicate that the dissociation of an H-radical has the energetically lowest lying transition state which is 39.8 kcal/mol above the 1,1-difluoroethyl radical ground state.

The next higher lying transition state is the one of the H-shift reaction (4). The energy difference between these two transition states amounts to 10.7 kcal/mol. This leads to the assumption that the dissociation of a hydrogen radical should be by far the most favorable reaction. However, it is not easy to predict the probability of a bond breakage between the two carbon atoms (3) since this reaction has no reverse barrier according to our calculations. Therefore, this reaction could possibly occur much more frequently than predicted by just watching at transition state energies.

Linear transit simulations performed using the GAUSSIAN 09 software did not result in any transition state for the loss of H₂ in one step, i.e. simultaneous breakage of two carbon-hydrogen bonds and formation of a hydrogen-hydrogen bond. Rather, we find a process corresponding to the hydrogen atom roaming mechanism for the loss of H₂³⁷⁻³⁹ and a transition state for the abstraction of the second H atom by the first one can be assigned. The treatment of roaming transition states is not simple. However, the calculated activation energy of this reaction of 20.6 kcal/mol indicates that this reaction channel is of only minor importance to the overall dissociation dynamics. The same is true for the elimination of H₂ from Product (9). Connecting lines between (1) and (2) as well as between (10) and (12) and (11) and (13) in Figure 5 are therefore displayed using a dotted line style.

As for the C-C bond breakage reactions of the products (0), (4) and (9) we did not find reverse barriers for fluorine radical dissociation reactions. Reactions (6) and (14) lead to the same product lying 53.4 kcal/mol above the ground state of 1,1-difluoroethyl radical.

A summary of the energetic results and a comparison between the energies calculated at HCTH147/6-31G** and CCSD(T)/cc-pVTZ levels of theory appears in Table I for reaction products and in Table II for transition states. Product (0), the ground state of 1,1-difluoroethyl radical serves as reference for the relative energies for all products and transition states. For most of the products, differences in relative energies comparing the two computational methods are less than 3-4 kcal/mol except where fluorine atoms are involved in the dissociation reactions (6), (7), (14), (15), (16). Furthermore, the substrate (0) as well as the reaction products (1), (3) and (4), which are considered to result from the most important reaction channels are investigated using UCCSD(T)/cc-pVTZ-F12 calculations. Energies of those structures all lie in between the values obtained by the CCSD(T)/cc-pVTZ and the DFT method and are given in Table I.

Differences in transition state energies relative to product (0) are generally larger than relative energies of reaction products. Most transition state energies are underestimated by the DFT method. Transition states of the H-shift reaction (0) → (4) lies about 3.1 kcal/mol higher and the F-shift reaction (4) → (9) is enhanced at about 5.8 kcal/mol using CCSD(T) instead of DFT. Largest differences occur in transition states that result in the loss of diatomic fragments such as H₂-elimination or HF-elimination. CCSD(T)-energies for all of them lie higher in energy at 6.1 – 9.4 kcal/mol than DFT-energies. However, a closer investigation on the transition states of the H dissociation reaction (0) → (1) and the H-shift reaction (0) → (4), determined at the UCCSD(T)/cc-pVTZ-F12 level of theory show, that their energies again lie in between the

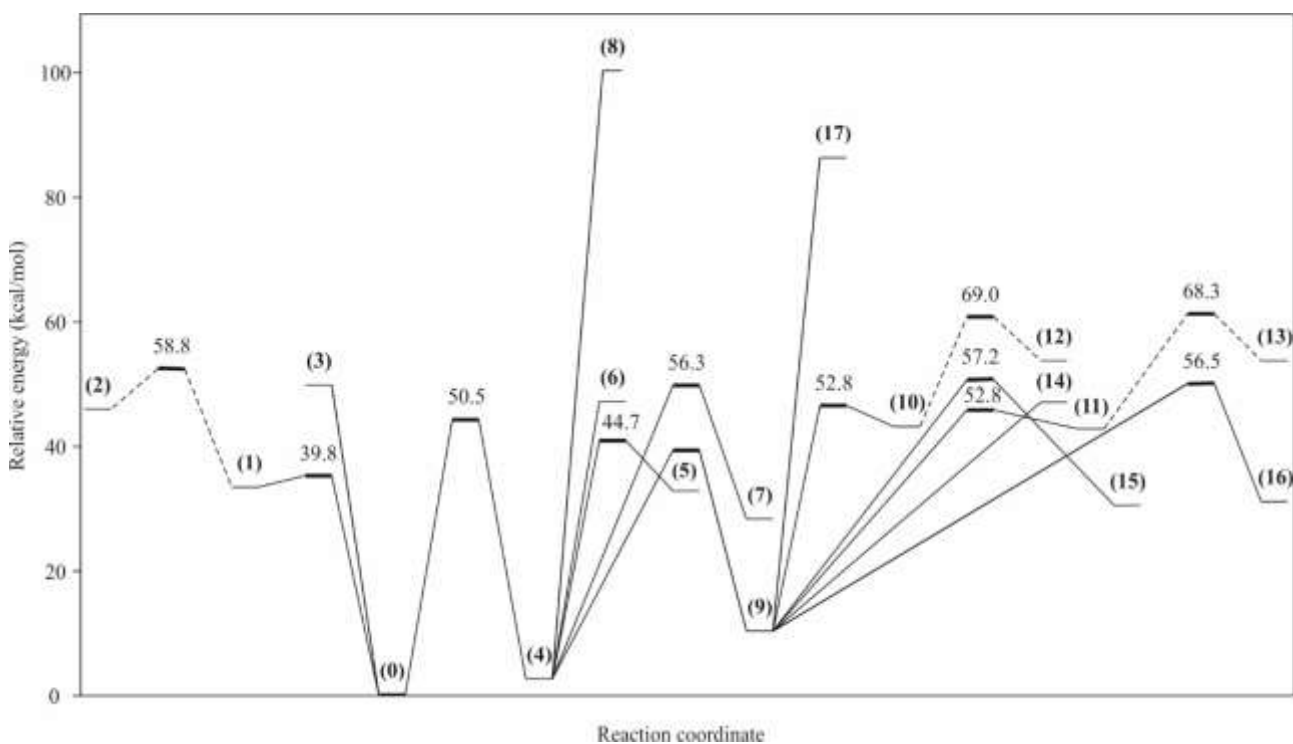


FIG. 5: Simplified energy surface of the dissociation reaction system of 1,1-difluoroethyl radical labeled as (0). Numbers in brackets indicate the corresponding reaction pathway. Transition state energies have a slightly broader line. The products of all processes are labeled in brackets and relative energies of transition states are given in kcal/mol. For the H₂-elimination reactions it is not clear which path on the energy surface is taken, therefore the connecting lines are displayed as dashed lines.

CCSD(T)/cc-pVTZ and the DFT-energies. The exact values are given in Table II.

In addition to the energies of structures given in Tables I & II and Figure 4, we calculate the transition state energies of rotational transition states of product (1), (4) and (9) as well as the other rotamer (enantiomer) of product (9). Calculations show that the two rotamers of (9) have very similar energies of 11.7 kcal/mol respectively. In addition to a rotation around the C-C bond, the one rotamer of (9) can also undergo an H-shift reaction to form the other enantiomer. We calculated the corresponding transition states and found them to be much too high in energy (58.9 kcal/mol and 63.4 kcal/mol respectively) to have significant contributions to the overall reaction dynamics.

TABLE I. Energies of all relevant reaction products in kcal/mol calculated at the HCTH147/6-31G** and the CCSD(T)/cc-pVTZ level of theory.

Reaction Product(s)	Relative Energy (HCTH147/6-31G**) (kcal/mol)	Relative Energy (CCSD(T)/cc-pVTZ) (kcal/mol)	Relative Energy (CCSD(T)/cc-pVTZ-F12) (kcal/mol)
(0)	0	0	0
(1)	39.4	38.2	38.9
(2)	49.1	51.4	-
(3)	59.6	56.4	58.2
(4)	6.7	2.9	2.9
(5)	39.4	38.2	38.9
(6)	64.5	53.4	-
(7)	39.6	32.3	-
(8)	120.2	114.4	-
(9)	13.8	11.7	-
(10)	50.8	48.5	-
(11)	50.8	48.8	-
(12)	56.3	59.7	-
(13)	56.4	59.7	-
(14)	64.5	53.4	-
(15)	44.4	35.7	-
(16)	44.4	35.0	-
(17)	100.9	97.4	-

TABLE II. Energies of transition states relative to reactant (0) calculated at the HCTH147/6-31G** and the CCSD(T)/cc-pVTZ level of theory in kcal/mol.

Transition state	Relative energy (HCTH147/6-31G**) (kcal/mol)	Relative energy (CCSD(T)/cc-pVTZ) (kcal/mol)	Relative energy (CCSD(T)/cc-pVTZ-F12) (kcal/mol)
(0) → (1)	42.2	39.8	40.0
(0) → (2)	52.6	58.8	-
(0) → (4)	47.4	50.4	49.8
(4) → (5)	46.5	44.7	-
(4) → (7)	46.9	56.3	-
(4) → (9)	37.5	43.3	-
(9) → (10)	55.2	52.8	-
(9) → (11)	55.3	52.8	-
(9) → (12)	62.4	69.0	-
(9) → (13)	61.9	68.2	-
(9) → (15)	48.1	56.5	-
(9) → (16)	48.9	57.2	-

Thus, it is to be expected that only a minor fraction of the 1,1-difluoroethyl radicals undergoes reactions other than (0) → (1), (0) → (3) and (0) → (4). Any other reaction (except (0) → (2)) can only occur after the formation of product (4) via H-shift.

B. Statistically derived rate constants and branching ratios - the prior distribution

We calculate the energy input for photodissociation reactions using the EOMCCSD/AUG-cc-pVDZ method as being the energy required for the excitation to the first excited state of the 1,1-difluoroethyl radical, which has 3s Rydberg character. The adiabatic excitation energy amounts to 94.8 kcal/mol. In the simplified PES given in Table I, all the reaction channels except C-C bond breakage reactions (8) and (17) should be accessible with such a high energy input. The input energy as well as relative energies and activation energies from the ground state PES derived by both methods, DFT and CCSD(T), serve as inputs to model the RRKM dissociation dynamics of the 1,1-difluoroethyl radical.

The roaming mechanism of H₂ loss is not simulated, because the RRKM treatment of such reactions is not accurate and the reaction channel is of minor importance to the overall reaction dynamics. Furthermore, in the spirit that the statistical treatment produces a prior distribution against which the BOMD-derived product distribution may be compared, one might argue that “special” transition states should not be handled explicitly in the RRKM calculation. Therefore, the fluorine atom dissociation channel was also not simulated.

Since the C-C bond breakage channel does not show a saddle point on the PES, such reactions are treated as loose transition states. **This treatment assumes a transition state at the centrifugal barrier and identical vibrational frequencies and internal rotational constants for the reaction products and the transition state.** It is questionable, whether the use of this approach is appropriate to model this reaction channel accurately. On the other hand, the statistical calculations, essentially phase space results, correspond to Levine’s prior distribution in surprisal theory, which define the expected distribution of products with no “other” effects. They provide a baseline against which the product distribution taken from the BOMD trajectory calculations, done with numerical energies and gradients, and no assumptions about symmetry or model (analytical) potential functions, may be assessed for new chemical information.

Figure 5 shows the fractions of reactant and products as a function of time and allows a comparison of the results based on ground state PESs derived based on the two different methods. For both methods, only the H-dissociation channel and the C-C bond breakage channel are drawn because the fractions of all the other reaction products are less than 2%. Although for some processes, the relative energies on the ground state PES show relatively large variations between different computational methods, the reaction dynamics and especially the branching ratios of both methods look quite similar. The decay of 1,1-difluoroethyl radical and the formation of dissociation products is somewhat slower in the model based on DFT-energies than for CCSD(T)-energies.

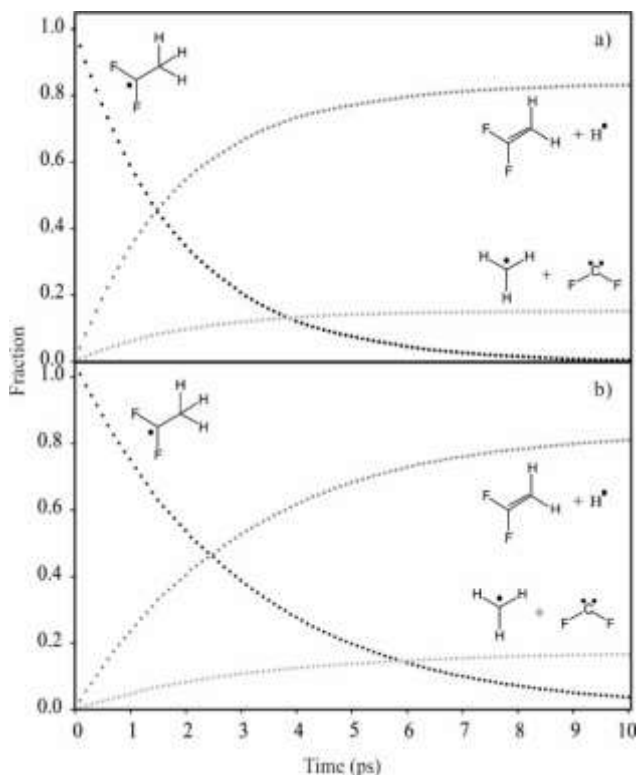


FIG. 6: Fractions of the 1,1-difluoroethyl radical and the main dissociation products as a function of time according a statistically treated photodissociation. a) Reaction dynamics is calculated based on CCSD(T)-energies. b) Reaction dynamics is calculated based on DFT-energies.

The branching ratios in both models are very similar. The fraction of CCSD(T)-energy based H dissociation products (1) is slightly higher and amounts to 83.2%. With the same model 15.2% C-C bond breakage products (3) are formed after 10 ps. The modeling based on DFT-energies yields a fraction of H dissociation products (1) that amounts to 77.6% and a fraction of C-C bond breakage products that is 15.9% after 10ps. After 10 ps, the 1,1-difluoroethyl radical is not fully decomposed and about 4% of reactant (0) remains undissociated in the DFT based model. Regarding the results described above and the circumstance that energies for all the relevant channels obtained by CCSD(T)-F12 calculations lie in between the energy values yielded by CCSD(T) and DFT, we think that the following assumptions are justified:

- Reaction channels other than H-dissociation and C-C bond breakage are of minor relevance to the overall reaction dynamics
- Branching ratios and reaction rates calculated at the CCSD(T)/cc-pVTZ and HCTH147/6-31G** level of theory can serve as upper and lower bounds of the value derived with the most accurate computational methods in a statistical RRKM approach.
- The HCTH147 functional reproduces energies derived by CCSD(T)-F12 very well. For the most relevant transition states, the largest deviation is less than 2.5 kcal/mol.

An overview of the results for the dissociation rate constants based on both methods as well as branching ratios are given in the next section in Tables III & IV.

C. Rate constants and branching ratios derived by BOMD-trajectories

We calculate 500 trajectories of the dissociation of 1,1-difluoroethyl radical. The excitation energy is the same as for the RRKM approach and amounts to 94.8 kcal/mol. Manual evaluation of the trajectories provides branching ratios for the dissociation products using the above-mentioned BOMD method. Table III gives an overview over the product fractions calculated using the different theoretical approaches.

As already the RRKM-derived branching ratios indicate, the 1,1-difluoroethyl radical decomposes mainly in H-radical dissociation and C-C bond breaking reactions. In this case, the branching ratio between H dissociation and C-C bond cleavage amounts to 4.88 and 5.47 respectively for DFT and CCSD(T) derived electronic surfaces. However, in contrast to what RRKM predicts, the BOMD-approach indicates that the C-C bond breakage is favored over the H dissociation. C-C bond cleavage occurs in 56% of all trajectories and H dissociation in only 38.4%, leading to a branching ratio of only 0.68. This trend is the opposite of what is shown by the statistically derived branching ratios. In 3.8% of all trajectories, we found that the H-shift reaction from reactant (0) to product (4) occurs. This is only slightly more than calculated by the RRKM model. In very few trajectories we observe (4) to react further to other products such as (7), (9), (11), (14), and (15). Six out of the 500 trajectories resulted in computational error due to convergence problems and are sorted out.

TABLE III. Fractions of products formed out of the reactant after 10 ps calculated statistically using energies at the HCTH147/6-31G** and CCSD(T)/cc-pVTZ level of theory as well as with MD at the HCTH147/6-31G** level.

Reaction product	RRKM at HCTH147/6-31G** (s ⁻¹)	RRKM at CCSD(T)/cc-pVTZ (s ⁻¹)	MD at HCTH147/6-31G** (s ⁻¹)
(0)	0.0354	0.0046	0.012
(1)	0.7763	0.8319	0.378
(2)	- ^{a)}	- ^{a)}	0.002
(3)	0.1591	0.1519	0.564
(4)	0.0012	0	0.014
(5)	- ^{b)}	- ^{b)}	0.004
(6)	0.0160	0.0113	0
(7)	0.0068	0.0003	0.014
(8)	- ^{a)}	- ^{a)}	0
(9)	0.0001	0	0.002
(10)	0.0006	0	0
(11)	0.0004	0	0.002
(12)	- ^{a)}	- ^{a)}	0
(13)	- ^{a)}	- ^{a)}	0
(14)	- ^{a)}	- ^{a)}	0.002
(15)	0.0027	0	0.006
(16)	0.0013	0	0
(17)	- ^{a)}	- ^{a)}	0

^{a)} H₂-elimination as well as F dissociation have not been taken into account in the RRKM calculations. ^{b)} (1) and (5) are the same product but originating from a different reactant. MultiWell gives the fraction of products only, not taking into account the reaction pathway.

Figure 6 shows the results for rate constants for the two major reaction channels. We selected trajectories leading to the dissociation of H-radicals and bond breaking between the two carbon atoms in the 1,1-difluoroethyl radical, and integrate the state probability in steps of 0.1 ps. The

resulting cumulative distributions of each reaction channel are drawn against time and fitted exponentially. We find that a single exponential describes the decomposition well enough. Calculated reaction rates amount to $5.1 \cdot 10^{11} \text{ s}^{-1}$ for the dissociation of an H-radical and $5.9 \cdot 10^{11} \text{ s}^{-1}$ for the C-C bond cleavage. This is in good accordance with literature values of C-H bond fission of 10^{11} - 10^{12} s^{-1} at 100-120 kcal/mol total excitation energy^{4, 12}. The fractions of dissociation reactions other than H dissociations and C-C bond cleavage are too small to make statistics and calculate the rate constants.

Table IV gives an overview over all the rate constants that are calculated in this work. For the H dissociation reaction, the two RRKM rate constants as well as the BOMD rate constant are in good agreement with each other. For the C-C bond breaking reactions we find that, no matter on which of the levels of theory the PES was modeled, RRKM-reaction rates are very similar. The rate constant we calculated using molecular dynamics is larger by a factor of 10. This also explains the difference in branching ratios between RRKM statistical method and the MD method since a larger rate constant leads to an enhanced fraction of C-C bond cleavage products.

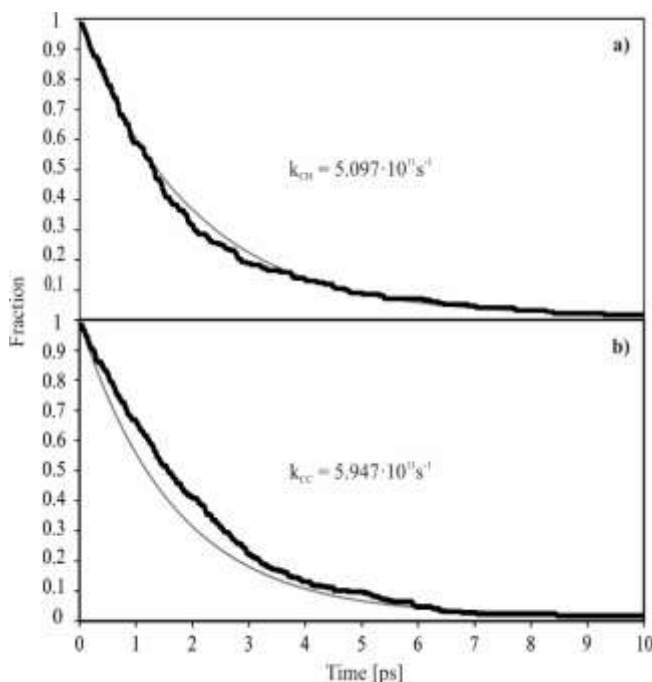


FIG. 7. a) Decay of the 1,1-difluoroethyl radical in a loss of H-radical. b) Decay of the 1,1-difluoroethyl radical due to carbon bond cleavage. The gray lines show exponential fits through the data points and the reaction rates k_{CH} and k_{CC} as multipliers of the time in the exponent is given in the middle of the figures.

TABLE IV. Reaction rates calculated using statistical methods (RRKM) at different levels of theory as well as reaction rates derived from trajectories at the HCTH147/6-31G** level of theory.

Reaction channel	RRKM at HCTH147/6-31G** (s ⁻¹)	RRKM at CCSD(T)/cc-pVTZ (s ⁻¹)	MD at HCTH147/6-31G** (s ⁻¹)
(0) → (1)	$2.66 \cdot 10^{11}$	$4.32 \cdot 10^{11}$	$5.10 \cdot 10^{11}$
(0) → (2)	- ^{a)}	- ^{a)}	-
(0) → (3)	$5.73 \cdot 10^{10}$	$8.14 \cdot 10^{10}$	$5.95 \cdot 10^{11}$
(0) → (4)	$1.30 \cdot 10^{10}$	$6.85 \cdot 10^9$	-
(4) → (5)	$9.08 \cdot 10^{10}$	$8.30 \cdot 10^{10}$	-
(4) → (6)	$2.07 \cdot 10^{11}$	$7.59 \cdot 10^{11}$	-
(4) → (7)	$1.24 \cdot 10^{11}$	$1.02 \cdot 10^{10}$	-

(4) → (8)	- ^{a)}	- ^{a)}	-
(4) → (9)	$2.05 \cdot 10^{11}$	$4.65 \cdot 10^{10}$	-
(9) → (10)	$8.59 \cdot 10^{10}$	$1.18 \cdot 10^{11}$	-
(9) → (11)	$9.80 \cdot 10^{10}$	$1.36 \cdot 10^{11}$	-
(9) → (12)	- ^{a)}	- ^{a)}	-
(9) → (13)	- ^{a)}	- ^{a)}	-
(9) → (14)	$9.24 \cdot 10^{11}$	$2.72 \cdot 10^{12}$	-
(9) → (15)	$4.75 \cdot 10^{11}$	$5.66 \cdot 10^{10}$	-
(9) → (16)	$3.07 \cdot 10^{11}$	$3.67 \cdot 10^{10}$	-
(9) → (17)	- ^{a)}	- ^{a)}	-

^{a)} Sequential H₂-elimination as well as F dissociation have not been taken into account in the RRKM calculations.

IV. DISCUSSION

The aim of this study was to study the photodissociation dynamics of the 1,1-difluoroethyl radical and to compare the results to our previous work on the ethyl radical. For a direct comparison, we therefore used the same methods and basis sets here for the determination of the PES. However, molecules containing fluorine substituents usually exhibit large polarization effects. For a good description of such molecules, it is important to use appropriate basis sets for our calculations and computations at the CBS limit should give the most reliable results. To check the influence of the basis set we perform single point calculations with larger basis sets and compare the resulting relative energies. A list of relative energies derived at HCTH147/6-31++G** and CCSD(T)/AUG-cc-pVTZ as well as a comparison to the methods with non-augmented basis sets is given in the appendix. Furthermore, we compare the relative energies for the most relevant reaction channels to single point calculations at the CCSD(T)/cc-pVTZ-F12 level of theory, as shown in Tables I & II. We find that for coupled cluster methods, the introduction of an augmented basis set does not change the relative energies much. On this level of theory, deviations of relative energies are mostly within the range of ± 2 kcal/mol. For the DFT methods, the difference in relative energies is a bit larger and for some reaction channels as high as 10 kcal/mol. However, reaction channels where large differences in relative energies occur are those where fluorine is involved in the reaction. Regarding the reaction scheme in Figure 1, such reactions only occur after an 1,2-H shift in the starting material and are therefore of minor importance. Furthermore, the energies calculated using CCSD(T)/cc-pVTZ-F12, at least for the relevant structures, all lie in between the energies obtained by CCSD(T)/cc-pVTZ and DFT (non-augmented). HCTH147/6-31G** thus reproduces CCSD(T)/cc-pVTZ-F12 even better than it reproduces CCSD(T)/cc-pVTZ. The rate constants that would be obtained by RRKM using CCSD(T)-F12 are expected therefore to lie between the values presented in Table IV. Furthermore, since the rate constants for the different potential energy surfaces differ only slightly in the RRKM approach, the HCTH147 functional seems to be appropriate to use for the BOMD trajectory calculations.

One must be careful with the comparison of the reaction rates and branching ratios between the different approaches discussed above. In RRKM modeled results, the decomposition is taking places on a fixed time scale and branching ratios are taken after 10 ps where the reaction is

not totally run to completion as seen in Figure 6 b). For the BOMD method, there is no time limit given and all trajectories (other than the 6 trajectories terminating due to a computational error) end up in one of the products. Nevertheless, it is seen that after 10 ps only a small fraction of surviving starting materials remains, which minimizes the error and in our opinion makes a comparison reasonable.

Statistical theories of chemical reactions treat photodissociation dynamics as thermal reactions of microcanonical ensembles, and assume a fast internal energy conversion to the ground state with redistribution of energy within the electronic ground state, which is much faster than the dissociation rate. Recent work questions the validity of this assumption in the dissociation dynamics of small alkyl radicals. Bach and Hostettler performed quasiclassical trajectory calculations on the same level of theory as used in this work to investigate the dissociation dynamics of the ethyl radical^{18, 19, 31}. As mentioned in the introduction, they found a fraction of ethyl radicals decaying much slower than expected, with rates of about 10^7 s^{-1} . Statistical rate theories such as RRKM would predict dissociation rates that are roughly four orders of magnitude larger, on the order of 10^{11} s^{-1} . A possible explanation of that result is a trapping of part of the population in highly excited torsional vibrational states. The weak coupling of these torsional excitations to other modes causes a bottleneck for the dissociation of hydrogen atoms. Steinbauer *et al.* support the finding of a channel of H-atoms formed with an unusually slow decay rate on the order of 10^7 s^{-1} in their velocity map imaging experiment⁴⁰. They suggest that interactions with a valence state play a role in the photodissociation and might explain the occurrence of a fraction of long-lived ethyl radicals. However, in this work, for the 1,1-difluoroethyl radical, we find no indications of a long living fraction of the reactant. In fact, the reaction rates for H dissociation obtained by trajectory calculations agree shockingly well with the value predicted by RRKM. A single exponential fit describes the H atom dissociation well and there is no evidence for nonstatistical behaviour in the photodissociation dynamics of the 1,1-difluoroethyl radical.

There are several works that focus on the dissociation dynamics of other small hydrocarbon radicals such as the 2-propyl radical or the *tert*-butyl radical. In a photofragment translational spectroscopy experiment, Negru *et al.*²⁰ found a branching ratio between loss of H atom and methyl radical from *tert*-butyl radicals of 1.1. As in our work, this was lower than expected for statistical dissociation on the ground state surface since the loss of H atoms should be favored due to a lower energy barrier. This and other indicators led to the assumption that, especially the methyl dissociation, but also the loss of H atoms must occur on an excited state surface causing a faster C-C bond cleavage. Noller and Fischer found that for 2-propyl radicals, the loss of H atoms is the most probable dissociation process proceeding with reaction rates on the order of 10^7 s^{-1} ⁴¹. For the 1-propyl radical, in contrast, they predicted the C-C bond cleavage and formation of methyl radical and ethane to be the most favorable dissociation reaction. Thus, there are other examples where the branching ratio between H dissociation and C-C bond cleavage lie on the C-C cleavage side.

In principle, one could attempt to ameliorate the discrepancy between the RRKM predicted reaction rate for the C-C bond cleavage channel, and the results of the BOMD simulation, by adding effects due to anharmonicity, or by implementing a variational transition state model for the description of the C-C bond cleavage channel, but the aim of the RRKM calculation was to provide the comparison against which the BOMD simulation can identify those places where a simple statistical treatment is inadequate. Accordingly, the discrepancy provides the motivation to explore additional models for that part of the potential surface involved in the C-C bond cleavage.

Beside H dissociation and C-C bond cleavage, we find other photodissociation processes occurring, but only to a small extent. In both theoretical approaches, RRKM as well as BOMD trajectory calculations, less than 7% of alternative products are formed. The fraction of trajectories resulting in one of the alternative products is not sufficient to derive rate constants, whereas RRKM calculations predict reaction rates in the order of 10^{10} to 10^{12} s^{-1} for these reactions. We consider them to be of minor importance to the overall dissociation dynamics.

V. CONCLUSIONS

We calculated reaction rates and branching ratios of several dissociation processes in the 1,1-difluoroethyl radical after photolytic excitation using RRKM theory as well as trajectory calculations. H dissociation yielding 1,1-difluoroethene and C-C bond cleavage leading to formation of methyl radicals and CF_2 emerge to be the most important processes both with reaction rates in the order of 10^{11} s^{-1} , which agrees very well with statistically derived dissociation rates of photolytically activated alkyl radicals. Trajectory calculations show a single exponential decay of the reactant towards both reaction channels and do not give any indication for nonstatistical effects for the H dissociation. The branching ratio between H dissociation and C-C bond is surprisingly low and amounts to 0.68 according to our trajectory calculations. RRKM computations provide much larger branching ratios. We assign the discrepancy to an underestimation of the C-C bond breakage rate constant using RRKM due to the lack of reverse barrier for the cleavage process and the use of non-scaled vibrational frequencies for the density of states computation.

SUPPLEMENTARY MATERIAL

See supplementary material for the geometries and absolute energies of all studied structures as well as the excited states of the difluoroethyl radicals and calculations including larger basis sets.

ACKNOWLEDGEMENTS

We gratefully acknowledge support of this work by the Schweiz. Nationalfonds and ETH Zürich.

1. G. Amaral, K. Xu and J. Zhang, *The Journal of Chemical Physics* **114** (12), 5164-5169 (2001).
2. J. L. Brum, S. Deshmukh and B. Koplitz, *The Journal of Chemical Physics* **93** (10), 7504-7505 (1990).
3. J. L. Brum, S. Deshmukh and B. Koplitz, *The Journal of Chemical Physics* **95** (3), 2200-2202 (1991).
4. T. Gilbert, T. L. Grebner, I. Fischer and P. Chen, *The Journal of Chemical Physics* **110** (12), 5485-5488 (1999).
5. G. W. Johnston, S. Satyapal, R. Bersohn and B. Katz, *The Journal of Chemical Physics* **92** (1), 206-212 (1990).
6. Z. Min, R. Quandt and R. Bersohn, *Chemical Physics Letters* **296** (3), 372-376 (1998).
7. R. Quandt, X. Wang, Z. Min, H. L. Kim and R. Bersohn, *The Journal of Physical Chemistry A* **102** (30), 6063-6067 (1998).
8. E. M. Evleth, H. Z. Cao, E. Kassab and A. Sevin, *Chemical Physics Letters* **109** (1), 45-49 (1984).
9. S. Matsika and D. R. Yarkony, *The Journal of Chemical Physics* **117** (15), 6907-6910 (2002).
10. A. Sevin, H. T. Yu and E. M. Evleth, *Journal of Molecular Structure: THEOCHEM* **104** (1), 163-178 (1983).
11. A. S. Zyubin, A. M. Mebel and S. H. Lin, *Chemical Physics Letters* **323** (5), 441-447 (2000).
12. W. L. Hase, G. Mrowka, R. J. Brudzynski and C. S. Sloane, *The Journal of Chemical Physics* **69** (8), 3548-3562 (1978).
13. W. L. Hase, R. J. Wolf and C. S. Sloane, *The Journal of Chemical Physics* **71** (7), 2911-2928 (1979).
14. W. L. Hase and D. G. Buckowski, *Journal of Computational Chemistry* **3** (3), 335-343 (1982).
15. W. L. Hase, D. G. Buckowski and K. N. Swamy, *The Journal of Physical Chemistry* **87** (15), 2754-2763 (1983).
16. W. L. Hase and H. B. Schlegel, *The Journal of Physical Chemistry* **86** (20), 3901-3904 (1982).
17. W. L. Hase, H. B. Schlegel, V. Balbyshev and M. Page, *The Journal of Physical Chemistry* **100** (13), 5354-5361 (1996).
18. A. Bach, J. M. Hostettler and P. Chen, *The Journal of Chemical Physics* **123** (2), 021101 (2005).
19. J. M. Hostettler, A. Bach and P. Chen, *The Journal of Chemical Physics* **130** (3), 034303 (2009).
20. B. Negru, G. M. P. Just, D. Park and D. M. Neumark, *Physical Chemistry Chemical Physics* **13** (18), 8180-8185 (2011).
21. J. R. Barker, *International Journal of Chemical Kinetics* **33** (4), 232-245 (2001).
22. J. R. Barker, *International Journal of Chemical Kinetics* **41** (12), 748-763 (2009).
23. J. R. Barker, T. L. Nguyen, J. F. Stanton, C. Aieta, M. Ceotto, F. Gabas, T. H. D. Kumar, C. G. L. Li, L. L. Lohr, A. Maranzana, N. F. Ortiz, J. M. Preses, J. M. Simmier, J. A. Sonk and P. J. Stimac, (University of Michigan, Ann Arbor, MI, 2011).
24. S. E. Stein and B. S. Rabinovitch, *The Journal of Chemical Physics* **58** (6), 2438-2445 (1973).
25. T. Beyer and D. F. Swinehart, *Commun. ACM* **16** (6), 379 (1973).
26. M. E. Weber, J. L. Elkind and P. B. Armentrout, *The Journal of Chemical Physics* **84** (3), 1521-1529 (1986).
27. K. M. Ervin and P. B. Armentrout, *The Journal of Chemical Physics* **83** (1), 166-189 (1985).
28. P. B. Armentrout and K. M. Ervin, (2002).
29. A. D. Boese, J. M. L. Martin and N. C. Handy, *The Journal of Chemical Physics* **119** (6), 3005-3014 (2003).
30. M. J. Frisch, G. W. Trucks, H. B. Schlegel, G. E. Scuseria, M. A. Robb, J. R. Cheeseman, G. Scalmani, B. Barone, B. Mennucci, G. A. Petersson, H. Nakatsuji, M. Caricato, X. Li, H. P. Hratchian, A. F. Izmaylov, J. Bloino, G. Zheng, J. L. Sonnenberg, M. Hada, M. Ehara, K. Toyota, R. Fukuda, J. Gasegawa, M. Ishida, T. Nakajima, Y. Honda, O. Kitao, H. Nakai, T. Vreven, J. J. A. Montgomery, J. E. Peralta, F. B. Ogliaro, M., J. J. Heyd, E. Brothers, K. N. Kudin, V. N. Staroverov, R. Kobayashi, J. Normand, K. Raghayachari, A. Rendell, J. C. Burant, S. S. Ivengar, J. Tomasi, M. Cossi, N. Rega, J. M. Millam, M. K. Klene, J. E., J. B. Cross, V. Bakken, C. Adamo, J. Jaramillo, R. Gomperts, R. E. Stratmann, O. Yazyev, A. J. Austin, R. Cammi, C. Pomelli, J. W. Ochterski, R. L. Martin, K. Morokuma, V. G. Zakrzewski, G. A. Voth, P. Salvador, J. J. Dannenberg, S. Dapprich, A. D. Daniels, O. Farkas, J. B. Foresman, J. V. Ortiz, J. Cioslowski and D. J. Fox, (2009), Vol. Revision A.1 (Gaussian, Inc., Wallingford CT, 2009).
31. A. Bach, J. M. Hostettler and P. Chen, *The Journal of Chemical Physics* **125** (2), 024304 (2006).
32. J. D. Watts, J. Gauss and R. J. Bartlett, *The Journal of Chemical Physics* **98** (11), 8718-8733 (1993).
33. J. F. Stanton, J. Gauss, M. E. Harding, P. G. Szalay, w. c. f. and A. A. Auer.
34. H.-J. K. Werner, P. J.; Knizia, G.; Manby, F. R. ; Schütz, M.; Celani, P.; Györffy, W.; Kats, D.; Korona, T.; Lindh, R.; Mitrushenkov, A.; Rauhut, G.; Shamasundar, K. R.; Adler, T. B.; Amos, R. D.; Bernhardsson, A.; Berning, A.; Cooper, D. L.; Deegan, M. J. O.; Dobbyn, A. J.; Eckert, F.; Goll, E.; Hampel, C.; Hesselmann, A.; Hetzer, G.; Hrenar, T.; Jansen, G.; Köppl, C.; Liu, Y.; Lloyd, A. W.; Mata, R. A.; May, A. J.; McNichols, S. J.; Meyer, W.; Mura, M. E.; Nicklass, A.; O'Neill, D. P.; Palmieri, P.; Peng, D.; Pflüger, K.; Pitzer, R.; Reiher, M.; Shiozaki, T.; Stoll, H.; Stone, A. J.; Tarroni, R.; Thorsteinsson, T. and Wang, M. , (2015).
35. H.-J. Werner, P. J. Knowles, G. Knizia, F. R. Manby and M. Schütz, *Wiley Interdisciplinary Reviews: Computational Molecular Science* **2** (2), 242-253 (2012).
36. G. A. Knizia, T. B.; Werner, H.-J., *The Journal of Chemical Physics* **130** (5), 054104 (2009).
37. A. M. Mebel, K. Morokuma and M. C. Lin, *The Journal of Chemical Physics* **103** (9), 3440-3449 (1995).
38. G.-S. Kim, T. L. Nguyen, A. M. Mebel, S. H. Lin and M. T. Nguyen, *The Journal of Physical Chemistry A* **107** (11), 1788-1796 (2003).

39. D. Townsend, S. A. Lahankar, S. K. Lee, S. D. Chambreau, A. G. Suits, X. Zhang, J. Rheinecker, L. B. Harding and J. M. Bowman, *Science* **306** (5699), 1158-1161 (2004).
40. M. Steinbauer, J. Giegerich, K. H. Fischer and I. Fischer, *The Journal of Chemical Physics* **137** (1), 014303 (2012).
41. B. Noller and I. Fischer, *The Journal of Chemical Physics* **126** (14), 144302 (2007).

Supporting Information

A) Geometries

A.1) Coordinates and vibrational frequencies

Coordinates and harmonical vibrational frequencies of all products and transition states are calculated at the HCTH147/6-31G** level of theory using structure optimization and frequency analysis. Results are given in the tables below.

1, 1-difluoroethyl radical (0)					
Atom	Coordinates [Å]			Harmonic frequencies [cm ⁻¹]	
	x	y	z		
C	0.064775	-1.491382	0.000000	201.6530	1238.6110
C	-0.305036	-0.046595	0.000000	201.6530	1257.8930
F	0.063236	0.633817	1.103608	365.7350	1391.5440
F	0.063236	0.633817	-1.103608	447.1720	1457.6220
H	1.159100	1.623219	0.000000	520.4530	2982.6700
H	-0.341229	-1.980192	0.890179	845.3050	3095.3630
H	-0.341229	-1.980192	-0.890179	967.7050	3142.2910
H				1074.6560	

1, 1-difluoroethene (1, 5)					
Atom	Coordinates [Å]			Harmonic frequencies [cm ⁻¹]	
	x	y	z		
C	0.144146	-0.000006	0.000000	429.2210	1319.2920
C	1.472265	-0.000032	0.000000	536.5260	1387.2540
F	-0.617147	1.088106	0.000000	614.3850	1761.4350
F	-0.617199	-1.088077	0.000000	701.8540	3191.1730
H	2.011070	-0.938671	0.000000	758.1630	3296.0190
H	2.011124	0.938570	0.000000	929.7630	
H				941.6700	

1, 1-difluoroethenyl radical (2)					
Atom	Coordinates [Å]			Harmonic frequencies [cm ⁻¹]	
	x	y	z		
C	0.116047	-0.135198	0.000000	407.6070	1227.4250
C	1.023423	-1.082687	0.000000	456.9340	1745.4720
F	-1.196368	-0.345169	0.000000	529.9590	3333.3170
F	0.365647	1.178505	0.000000	604.3990	
H	2.092343	-1.207977	0.000000	726.9610	
H				948.4480	

methyl radical (3)					
Atom	Cartesian coordinates [Å]			Harmonic frequencies [cm ⁻¹]	
	x	y	z		
C	0.000000	0.000000	-0.000002	456.4170	3291.7140
H	0.000000	-0.938872	0.542075	1389.3950	
H	0.000000	0.938872	0.542075	1389.5100	
H	0.000000	0.000000	-1.084124	3106.1320	
H	0.000000	0.000000	-1.084124	3291.9290	

CF ₂ (3)					
Atom	Cartesian coordinates [Å]			Harmonic frequencies [cm ⁻¹]	
	x	y	z		
C	0.000000	0.000000	0.618588	635.7100	
F	0.000000	1.042460	-0.195360	1097.7420	
F	0.000000	-1.042460	-0.195360		

1, 1-difluoroethyl radical (4)					
Atom	Coordinates [Å]			Harmonic frequencies [cm ⁻¹]	
	x	y	z		
C	0.000001	0.065544	0.355018	82.6800	1134.0530
C	0.000019	1.472231	-0.105107	382.7000	1344.1610
F	0.939401	2.007988	-0.191833	425.2490	1366.5930
F	-0.939349	2.008012	-0.191833	485.7260	1430.2300
H	-0.000001	-0.039650	1.457257	631.0670	2938.3100
H	-1.116637	-0.591108	-0.107402	895.2310	3160.6120
H				966.2700	3280.6920

H	1.116621	-0.591136	-0.107402	1124.4000
---	----------	-----------	-----------	-----------

monofluoroethene (6, 14)					
Atom	Coordinates [Å]			Harmonic frequencies [cm ⁻¹]	
	x	y	z		
C	-0.123009	-0.445685	0.000000	476.7830	1398.6330
C	-1.276815	0.215379	0.000000	719.1230	1702.0350
F	1.071946	0.175687	0.000000	827.2590	3153.9630
H	-0.018114	-1.530409	0.000000	928.9940	3171.7050
H	-1.312507	1.300710	0.000000	947.6680	3261.7750
H	-2.209044	-0.339941	0.000000	1168.7290	
H				1317.5690	

monofluoroethenyl radical (7)					
Atom	Coordinates [Å]			Harmonic frequencies [cm ⁻¹]	
	x	y	z		
C	-1.304834	-0.154761	0.000000	438.6710	1697.2710
C	-0.113341	0.419699	0.000000	604.2570	3108.6340
F	1.087328	-0.125889	0.000000	774.0210	3239.4180
H	-1.412357	-1.240972	0.000000	928.3020	
H	-2.198782	0.459519	0.000000	1149.1200	
H				1374.8140	

difluoromethyl radical (8)					
Atom	Cartesian coordinates [Å]			Harmonic frequencies [cm ⁻¹]	
	x	y	z		
C	0.000281	0.502847	-0.077484	528.498	3053.954
F	1.129382	-0.193182	0.015222	1003.524	
F	-1.123323	-0.202293	0.013138	1160.207	
H	-0.117563	1.467762	0.387974	1176.803	
H				1335.292	

CH ₂ (8)					
Atom	Cartesian coordinates [Å]			Harmonic frequencies [cm ⁻¹]	
	x	y	z		
C	0.000000	0.000000	0.096472	1416.2310	
H	0.000000	-0.859136	-0.574337	2809.9560	
H	0.000000	0.859136	-0.574337		

1, 2-difluoroethyl radical (9, rotamer a)					
Atom	Coordinates [Å]			Harmonic frequencies [cm ⁻¹]	
	x	y	z		
C	0.645584	0.564267	0.327427	122.6600	1245.5630
C	-0.662584	0.509770	-0.338873	300.3550	1350.2790
F	1.526072	-0.444604	-0.125150	445.4950	1423.1500
F	-1.557692	-0.381959	0.123342	574.6810	1461.3470
H	0.522912	0.440020	1.412405	900.0060	3012.0590
H	-0.843158	0.817455	-1.367406	933.9540	3069.7010
H	1.118723	1.535600	0.125365	1100.0120	3171.5120
H				1210.2600	

1, 2-difluoroethyl radical (9, rotamer b)					
Atom	Coordinates [Å]			Harmonic frequencies [cm ⁻¹]	
	x	y	z		
C	-0.645579	0.564262	0.327429	122.6540	1245.5650
C	0.662586	0.509766	-0.338874	300.3530	1350.2780
F	1.557695	-0.381958	0.123341	445.4910	1423.1520
F	-1.526081	-0.444598	-0.125151	574.6670	1461.3460
H	-1.118717	1.535601	0.125387	900.0070	3012.0610
H	0.843171	0.817466	-1.367400	933.9510	3069.7050
H	-0.522899	0.439992	1.412403	1100.0110	3171.5140
H				1210.2670	

<i>cis</i> -1, 2-difluoroethene (10)					
Atom	Coordinates [Å]			Harmonic frequencies [cm ⁻¹]	
	x	y	z		
C	-0.667131	0.638631	0.000000	223.4390	1276.1670
C				487.2040	1388.8460

C	0.667100	0.638659	0.000000	759.9070	1750.2960
F	-1.399700	-0.486075	0.000000	767.0530	3181.0820
F	1.399734	-0.486055	0.000000	802.8550	3205.8400
H	-1.246636	1.558423	0.000000	1015.4920	
H	1.246347	1.558635	0.000000	1145.9330	

<i>trans</i> -1, 2-difluoroethene (11)					
Atom	Coordinates [Å]			Harmonic frequencies [cm ⁻¹]	
	x	y	z		
C	-0.529010	0.406333	0.000000	310.4010	1284.6000
C	0.529006	-0.406307	0.000000	333.8880	1287.0570
F	-1.777237	-0.097637	0.000000	547.2710	1733.8460
F	1.777243	0.097619	0.000000	762.4350	3191.6450
H	1.777243	0.097619	0.000000	892.9320	3199.2830
H	-0.476809	1.492237	0.000000	1153.4810	
H	0.476747	-1.492209	0.000000	1181.0060	

<i>cis</i> -1, 2-difluoroethenyl radical (12)					
Atom	Coordinates [Å]			Harmonic frequencies [cm ⁻¹]	
	x	y	z		
C	0.670900	0.635163	0.000000	202.1390	1338.3130
C	-0.655833	0.615056	0.000000	370.5250	1742.9420
F	-1.505868	-0.385501	0.000000	733.9520	3219.1510
F	-1.505868	-0.385501	0.000000	766.2480	
F	1.430999	-0.487127	0.000000	1005.6120	
H	1.231952	1.563672	0.000000	1126.3170	

<i>trans</i> - 1, 2 -difluoroethenyl radical (13)					
Atom	Coordinates [Å]			Harmonic Frequencies [cm ⁻¹]	
	x	y	z		
C	0.543054	-0.400568	0.000000	292.4800	1280.1020
C	-0.545275	0.360228	0.000000	298.2310	1729.5080
F	-1.801608	-0.032757	0.000000	537.2310	3133.8690
F	-1.801608	-0.032757	0.000000	663.5400	
F	1.775252	0.137366	0.000000	1120.1970	
H	0.523283	-1.491655	0.000000	1202.7490	

<i>cis</i> -monofluoroethenyl radical (15)					
Atom	Coordinates [Å]			Harmonic Frequencies [cm ⁻¹]	
	x	y	z		
C	0.154435	-0.431294	0.000000	418.4200	1655.7290
C	1.326097	0.158855	0.000000	594.9340	3153.5240
F	-1.028591	0.192055	0.000000	780.8870	3298.7560
H	0.002528	-1.520754	0.000000	865.5510	
H	0.002528	-1.520754	0.000000	1044.8500	
H	1.758905	1.144229	0.000000	1291.8340	

<i>trans</i> -monofluoroethenyl radical (16)					
Atom	Coordinates [Å]			Harmonic frequencies [cm ⁻¹]	
	x	y	z		
C	0.168257	0.409568	0.000000	465.6490	1670.4490
C	1.293644	-0.268106	0.000000	597.7410	3085.6590
F	0.102531	1.502928	0.000000	733.8410	3295.5210
H	-1.053638	-0.165915	0.000000	782.6830	
H	-1.053638	-0.165915	0.000000	1108.8690	
H	2.352876	-0.059644	0.000000	1277.9110	

monofluoromethyl radical (17)					
Atom	Cartesian coordinates [Å]			Harmonic frequencies [cm ⁻¹]	
	x	y	z		
C	-0.057495	0.740239	0.000000	604.832	3241.707
F	0.009897	-0.599338	0.000000	1165.278	
H	0.249006	1.242080	0.910316	1189.745	
H	0.249006	1.242080	-0.910316	1470.524	
H	0.249006	1.242080	-0.910316	3092.143	

CFH (17)					
----------	--	--	--	--	--

Atom	Cartesian coordinates [Å]			Harmonic frequencies [cm ⁻¹]	
	x	y	z		
C	-0.771095	-0.099250	0.000000	1195.7000	
F	0.546697	0.013255	0.000000	1422.1510	
H	-1.124428	0.931893	0.000000		

hydrogen molecule (1, 5, 10, 11)					
Atom	Cartesian coordinates [Å]			Harmonic frequencies [cm ⁻¹]	
	x	y	z		
H	0.000000	0.000000	0.371830	4437.7181	
H	0.000000	0.000000	-0.371830		

hydrogenfluoride (7, 15, 16)					
Atom	Cartesian coordinates [Å]			Harmonic frequencies [cm ⁻¹]	
	x	y	z		
F	0.000000	0.000000	0.046558	4059.2144	
H	0.000000	0.000000	-0.877664		

TS H dissociation (0 -> 1)					
Atom	Cartesian coordinates [Å]			Harmonic frequencies [cm ⁻¹]	
	x	y	z		
				146.1860	945.8130
C	-0.166696	-1.433836	0.000000	170.4130	1330.2970
C	-0.051168	-0.105041	0.000000	428.5610	1387.1380
F	0.026516	0.647733	-1.087722	537.9260	1726.1810
F	0.026516	0.647733	1.087722	608.7150	3195.4640
H	2.104031	-2.166858	0.000000	729.3480	3302.2330
H	-0.254837	-1.965352	0.938308	778.9480	-331.4080
H	-0.254837	-1.965352	-0.938308	929.7310	

TS H shift (0 -> 4)					
Atom	Cartesian coordinates [Å]			Harmonic frequencies [cm ⁻¹]	
	x	y	z		
				188.3260	1291.7720
C	-0.081888	1.509437	0.000000	385.9940	1299.2830
C	0.225474	0.072867	0.000000	458.0590	1396.3950
F	-0.059235	-0.630995	1.119228	599.1370	2102.3860
F	-0.059235	-0.630995	-1.119228	679.7800	3150.3010
H	1.165984	0.979458	0.000000	898.9900	3285.6260
H	-0.321189	1.984970	-0.945018	909.7390	-2005.5340
H	-0.321189	1.984970	0.945018	1177.8320	

TS H ₂ elimination (1 -> 2)					
Atom	Cartesian coordinates [Å]			Harmonic frequencies [cm ⁻¹]	
	x	y	z		
				166.9630	926.6660
C	-1.132236	-0.864639	0.000002	228.7840	1047.1030
C	-0.062655	-0.092228	0.000001	481.0140	1254.0940
F	-0.079084	1.234975	0.000001	532.3930	1727.3050
F	1.198718	-0.529987	-0.000001	537.6520	2508.3500
H	-1.215537	-1.941185	0.000003	619.9270	3283.9780
H	-2.455145	-0.164820	-0.000008	835.5400	-712.2100
H	-3.208061	0.209593	-0.000015	862.8850	

TS H dissociation (4 -> 5)					
Atom	Cartesian coordinates [Å]			Harmonic frequencies [cm ⁻¹]	
	x	y	z		
				374.1250	948.6620
C	0.047453	0.125201	0.000000	448.3170	1331.2800
C	-0.070408	1.481684	0.000000	455.3550	1381.6090
F	-0.043309	-0.619447	1.092969	544.4830	1605.9790
F	-0.043309	-0.619447	-1.092969	634.4400	3180.0270
H	-0.058804	2.012674	-0.944129	650.0840	3296.6590
H	-0.058804	2.012674	0.944129	749.1510	-773.0580
H	2.023751	0.196008	0.000000	908.1290	

TS HF elimination (4 -> 7)					
Atom	Cartesian coordinates [Å]			Harmonic frequencies [cm ⁻¹]	
	x	y	z		
C	-0.363055	0.100333	-0.197209	114.2500	1229.0440
C	-0.860036	1.323304	0.061982	220.7130	1377.5310
F	1.871803	-0.067832	0.052993	489.2670	1593.0900
F	-1.022484	-1.021680	0.053590	607.4380	2347.7150
H	-1.903995	1.466116	0.331219	757.7550	3153.6740
H	-0.218924	2.186585	-0.077488	850.3960	3267.9620
H	0.675627	-0.065423	-0.652794	936.0180	-428.0960
H				1156.6530	

TS F shift (4 -> 9)					
Atom	Cartesian coordinates [Å]			Harmonic frequencies [cm ⁻¹]	
	x	y	z		
C	0.447696	0.258001	0.468617	185.8060	1295.2650
C	-0.378381	1.130968	-0.180929	361.2030	1405.1800
F	-1.386166	-0.634877	-0.033242	471.8920	1605.3560
F	1.390887	-0.406705	-0.184224	665.9120	3176.4390
H	-0.293042	1.280094	-1.251782	794.1130	3204.1390
H	-1.072507	1.739473	0.385451	869.5480	3289.4870
H	0.451231	0.076956	1.540325	942.0150	-322.1570
H				1200.7200	

TS H dissociation (9 -> 10)					
Atom	Cartesian coordinates [Å]			Harmonic frequencies [cm ⁻¹]	
	x	y	z		
C	-0.670551	-0.608490	-0.078919	218.1510	1155.3940
C	0.676678	-0.625971	-0.108823	251.8050	1270.7010
F	-1.257771	-1.494698	-0.303812	321.8460	1393.2360
F	1.411819	0.477698	0.057879	504.1010	1680.4810
H	-1.365001	0.533094	-0.014489	755.7460	3188.0620
H	1.244078	-1.548835	-0.195575	764.3820	3209.2450
H	-0.941823	-1.312294	1.916868	845.1970	-500.6190
H				1014.3150	

TS H dissociation (9 -> 11)					
Atom	Cartesian coordinates [Å]			Harmonic frequencies [cm ⁻¹]	
	x	y	z		
C	-0.528592	-0.376833	0.126844	250.9590	1191.7250
C	-1.764173	0.135741	0.018528	292.4190	1271.4390
F	0.541100	0.406904	-0.109326	339.2890	1288.5430
F	-0.475877	-1.365734	0.574239	352.6540	1669.0220
H	0.490032	1.425455	-0.485600	545.8340	3195.4630
H	1.780123	-0.075840	0.055091	764.9990	3200.3730
H	-0.463752	-1.546964	-1.684994	895.8270	-483.2980
H				1156.5170	

TS H ₂ elimination (10 -> 12)					
Atom	Cartesian coordinates [Å]			Harmonic frequencies [cm ⁻¹]	
	x	y	z		
C	0.533598	-0.315221	-0.000001	232.9670	1125.8570
C	-0.552016	0.454941	0.000001	240.5880	1193.8210
F	-1.783501	-0.083015	0.000000	315.2230	1278.2920
F	1.779545	0.143077	0.000000	327.9660	1709.7790
H	-0.532185	1.544900	0.000001	545.7460	1964.5380
H	0.432552	-1.727695	0.000000	732.6970	3149.2040
H	0.393501	-2.613051	0.000003	971.3470	-940.7750
H				1100.9410	

TS H ₂ elimination (10 -> 13)					
Atom	Cartesian coordinates [Å]			Harmonic frequencies [cm ⁻¹]	
	x	y	z		
C	0.671275	-0.505172	0.000000	204.1200	1120.8690
C	-0.652631	-0.639193	0.000000	210.3970	1180.9570
F	-1.503988	0.407705	0.000000	264.6390	1339.3550
F	-1.130632	-1.614316	0.000000	414.2640	1723.0930
H	1.371194	0.618179	0.000000	721.1870	1965.5070
H	1.458751	-1.681336	0.000000	773.4760	3204.8360
H				927.8140	-938.7340

H	1.953178	-2.417416	0.000001	995.8440
---	----------	-----------	----------	----------

TS HF elimination (9 -> 15)					
Atom	Cartesian coordinates [Å]			Harmonic frequencies [cm ⁻¹]	
	x	y	z		
C	-0.199837	-0.685300	0.096858	229.4360	1300.5840
C	0.704617	0.301920	0.114636	388.1020	1606.4260
F	-2.281970	0.198447	-0.071124	547.3230	1874.5590
F	2.008786	0.082971	-0.089014	769.3660	3182.0070
H	-0.043127	-1.684002	-0.301768	871.3010	3209.5080
H	0.478081	1.342621	0.341834	948.2410	-572.4910
H	-1.295525	-0.398759	0.460452	1149.3040	

TS HF elimination (9 -> 16)					
Atom	Cartesian coordinates [Å]			Harmonic frequencies [cm ⁻¹]	
	x	y	z		
C	-0.168135	1.017858	-0.112729	271.1380	1300.4010
C	1.056818	0.520444	0.102711	502.5590	1622.8960
F	-1.938830	-0.387545	0.046054	551.1140	1995.4030
F	1.352591	-0.769695	-0.037622	722.1030	3132.2210
H	1.935540	1.127557	0.333408	897.7450	3221.1300
H	-0.435363	2.034633	0.158952	926.4250	-541.6520
H	-1.030451	0.336536	-0.532034	1144.0380	

TS rotation (0 -> 0)					
Atom	Cartesian coordinates [Å]			Harmonic frequencies [cm ⁻¹]	
	x	y	z		
C	1.504660	0.000003	0.063885	389.5440	1378.8240
C	0.047140	0.000000	-0.296963	474.6280	1447.5380
F	-0.639483	-1.102840	0.061151	518.2740	1467.8600
F	-0.639489	1.102837	0.061151	847.6230	3019.5100
H	1.747516	0.892939	0.650584	929.5760	3097.4480
H	1.747520	-0.892933	0.650583	1014.8210	3120.5020
H	2.137711	0.000004	-0.831424	1233.8570	-211.5930
H				1258.1110	

TS rotation (4 -> 4)					
Atom	Cartesian coordinates [Å]			Harmonic frequencies [cm ⁻¹]	
	x	y	z		
C	-0.078980	0.000007	0.372719	340.9570	1340.5220
C	-1.472665	0.000116	-0.115819	458.2910	1377.3660
F	0.595092	1.106496	-0.103772	545.9990	1448.5870
F	0.594919	-1.106588	-0.103772	551.1080	3033.6460
H	-1.651121	0.000111	-1.186767	878.3180	3155.9080
H	-2.312197	0.000147	0.571042	1019.2260	3276.4840
H	0.005720	0.000001	1.469267	1109.2010	-106.3530
H				1136.2990	

TS H-shift a (9 -> 9)					
Atom	Cartesian coordinates [Å]			Harmonic frequencies [cm ⁻¹]	
	x	y	z		
C	-0.685929	0.617619	0.167368	257.6600	1216.8860
C	0.734992	0.636955	-0.156469	364.5500	1385.5620
F	1.427129	-0.513360	0.057571	436.9580	1431.7150
F	-1.472029	-0.481267	-0.072910	693.0170	2054.1920
H	1.217682	1.291631	-0.891773	845.5970	3151.8540
H	0.242616	0.952562	1.047772	1003.4340	3163.1490
H	-1.198087	1.567398	0.003385	1052.9000	-1873.4240
H				1211.9480	

TS H-shift b (9 -> 9)					
Atom	Cartesian coordinates [Å]			Harmonic frequencies [cm ⁻¹]	
	x	y	z		
C	-0.621302	-0.349175	-0.366067	174.7900	1278.3860
C	0.621310	-0.348959	0.366264	353.1380	1313.3940
F	1.748437	0.279344	-0.107598	602.3170	1425.0050
F				735.5860	2078.1260

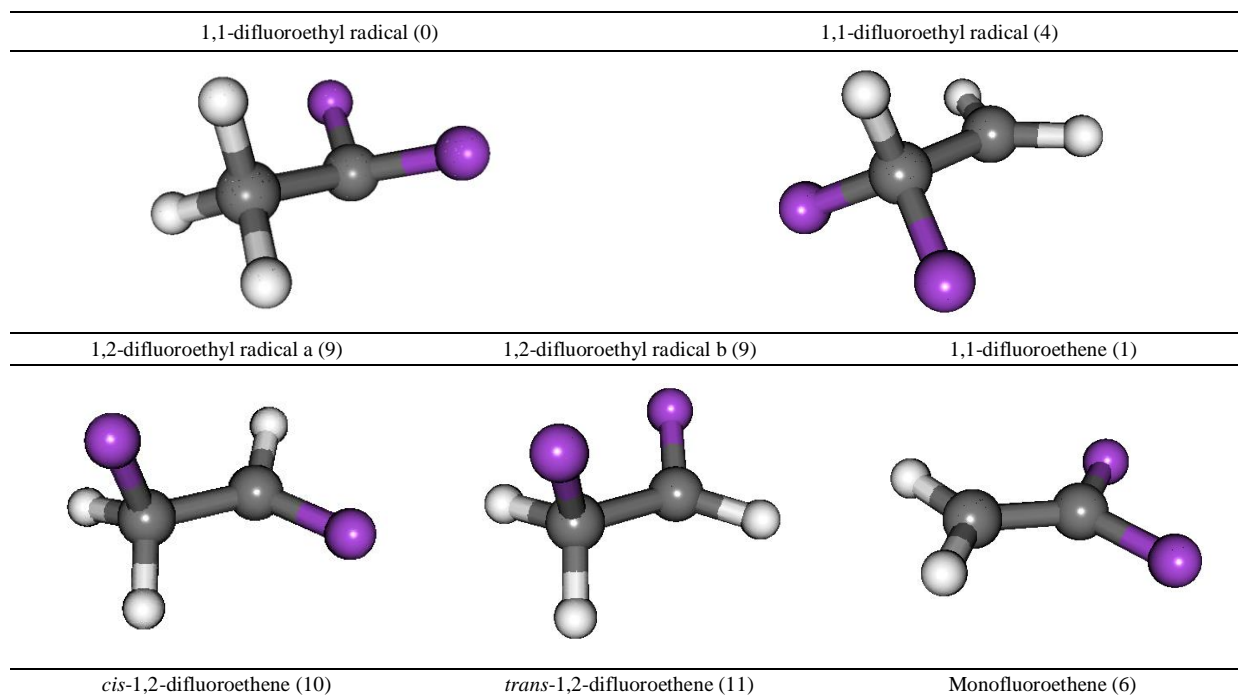
F	-1.748441	0.279407	0.107439	788.2320	3046.0700
H	0.573929	-0.372915	1.454899	950.2510	3132.3710
H	-0.000004	-1.473658	0.000436	1086.0110	-1963.0860
H	-0.573932	-0.373816	-1.454685	1194.8060	

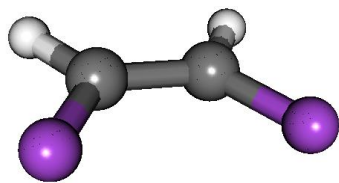
TS rotation a (9 -> 9)					
Atom	Cartesian coordinates [Å]			Harmonic frequencies [cm ⁻¹]	
	x	y	z		
C	-0.572846	0.526394	-0.124160	310.1730	1305.8530
C	0.572830	-0.421203	-0.237202	356.3740	1419.0430
F	-1.739562	-0.183936	0.122010	498.4930	1477.2440
F	1.774529	0.071606	0.129377	960.6940	2946.2000
H	1.774529	0.071606	0.129377	1059.6300	2977.6360
H	-0.724545	1.119797	-1.043672	1065.7400	3173.6890
H	0.451520	-1.493478	-0.092670	1177.7710	-126.6200
H	-0.385939	1.238724	0.700156	1201.5900	

TS rotation b (9 -> 9)					
Atom	Cartesian coordinates [Å]			Harmonic frequencies [cm ⁻¹]	
	x	y	z		
C	0.765036	-0.701391	0.017566	238.9350	1387.9810
C	-0.734037	-0.693479	0.031186	422.6100	1389.7170
F	1.264206	0.585163	-0.016734	657.9530	1482.2460
F	-1.336032	0.506797	0.003346	907.1630	2928.5500
H	-1.336032	0.506797	0.003346	971.5650	2951.1240
H	1.144834	-1.261026	-0.858648	1100.1770	3153.3980
H	-1.327861	-1.506999	-0.384246	1193.3760	-217.1270
H	1.167918	-1.207922	0.914790	1216.5540	

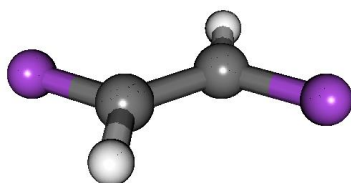
A.2) Images of reaction products and transition states

The images below show the structures of all products and transition states including a labeling of atoms within the structures that make the data for bond lengths, angles and dihedral angles readable.

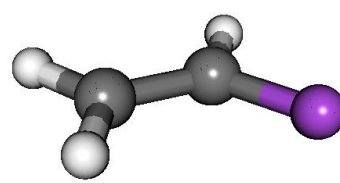




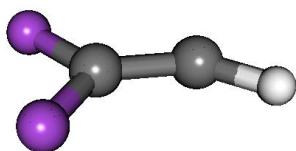
1,1-difluoroethenyl radical (2)



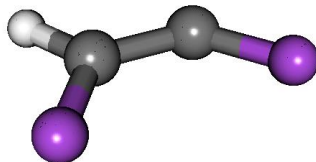
cis-1,2-difluoroethenyl radical (12)



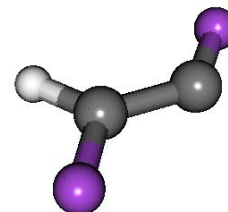
trans-1,2-difluoroethenyl radical (13)



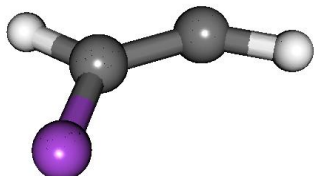
cis-monofluoroethenyl radical (15)



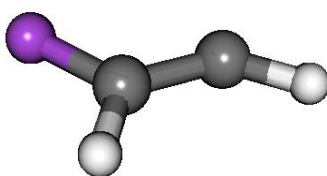
trans-monofluoroethenyl radical (16)



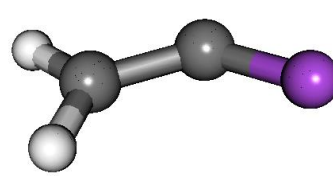
monofluoroethenyl radical (7)



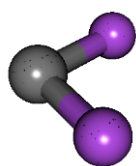
CF₂ (3)



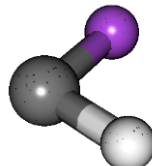
CHF (17)



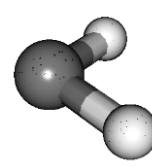
CH₂ (8)



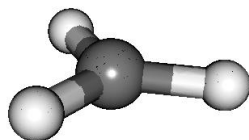
methyl radical (3)



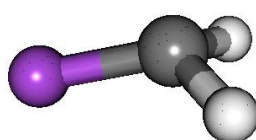
monofluoromethyl radical (17)



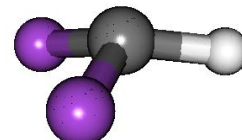
difluoromethyl radical



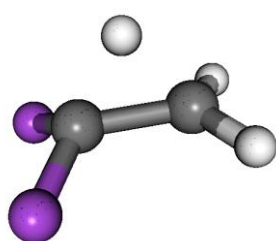
TS H shift (0 -> 4)



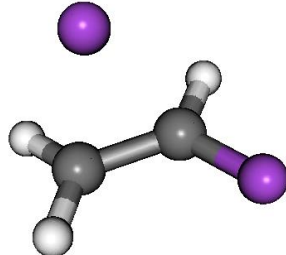
TS F shift (4 -> 9)



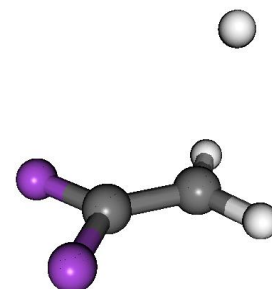
TS H dissociation (0 -> 1)



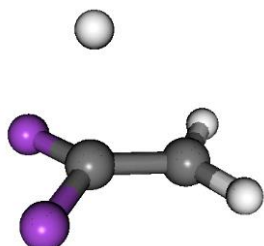
TS H dissociation (4 -> 5)



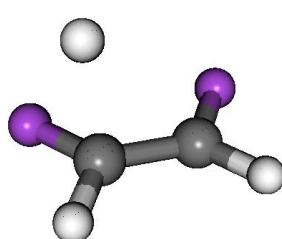
TS H dissociation (9 -> 10)



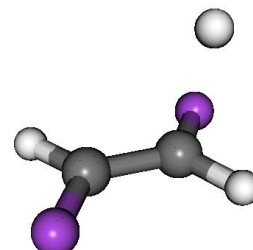
TS H dissociation (9 -> 11)



TS H₂ elimination (1 -> 2)



TS H₂ elimination (9 -> 13)



TS H₂ elimination (9 -> 12)

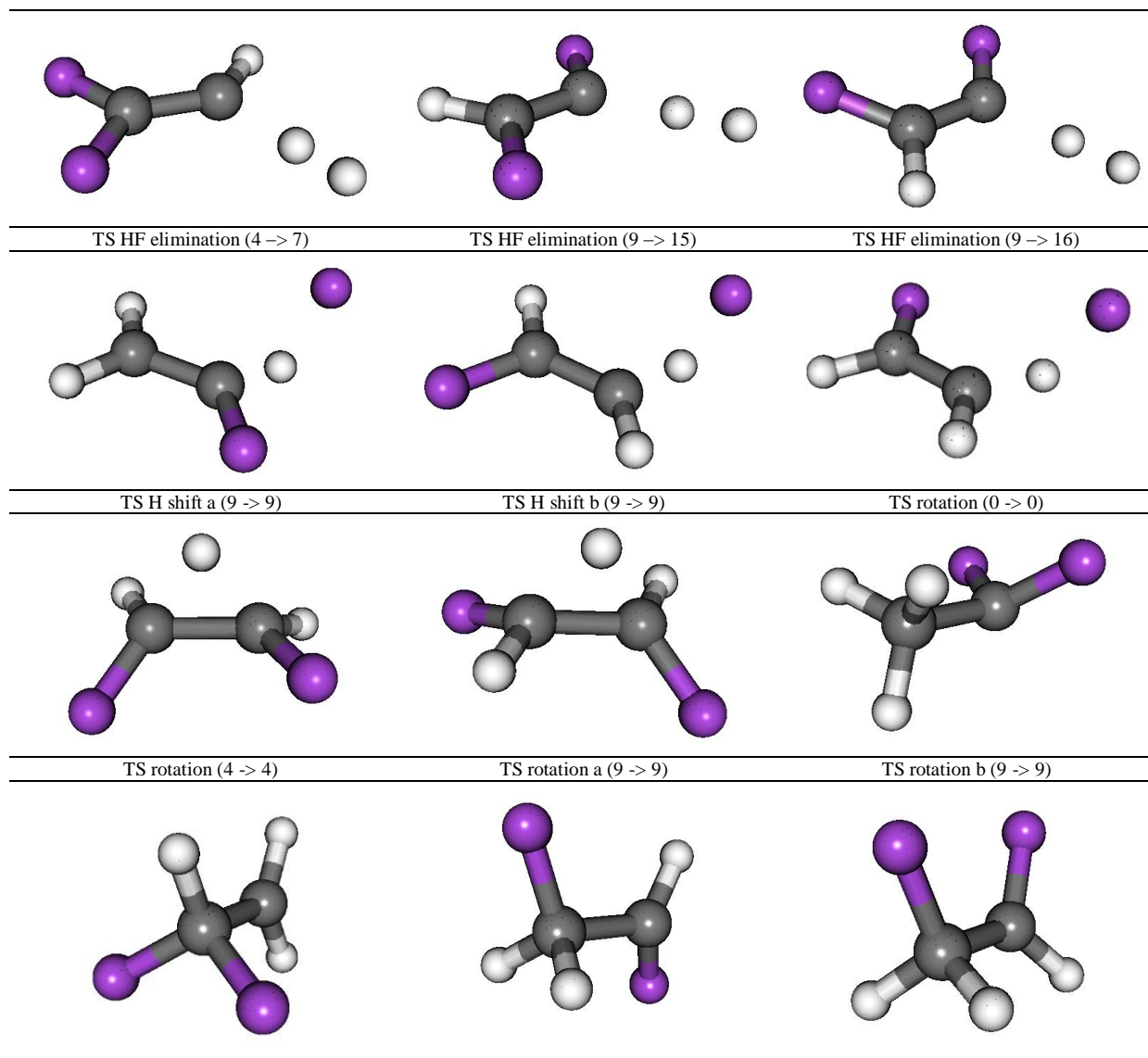


FIG. 1: images of all products and transition states discussed in this work based on HCTH147/6-31G** geometry optimization calculations.

A.3) Bond lengths:

Bond lengths between selected atoms within all structures are listed in the tables below. The atom labeling refers to the images in Fig.1.

Product	C _a -C _b	C _a -F _b	C _b -F _a	C _b -F _b	C _a -H _a	C _a -H _b	C _a -H _c	C _b -H _b	C _b -H _c
1,1-difluoroethyl radical (0)	1.49		1.35	1.35	1.10	1.09	1.09		
1,1-difluoroethyl radical (4)	1.48	1.38		1.37	1.11			1.08	1.08
1,2-difluoroethyl radical a (9)	1.47	1.35		1.41	1.10	1.10			1.09
1,2-difluoroethyl radical b (9)	1.47	1.41		1.35	1.10	1.10			1.09

Product	C _a -C _b	C _a -F _a	C _a -F _b	C _b -F _a	C _b -F _b	C _a -H _a	C _a -H _b	C _b -H _b	C _b -H _c
1,1-difluoroethene (1)	1.33			1.33	1.33	1.08	1.08		
<i>cis</i> -1,2-difluoroethene (10)	1.33	1.34				1.34	1.09	1.09	
<i>trans</i> -1,2-difluoroethene (11)	1.33	1.35				1.35	1.05	1.09	
Monofluoroethene (6, 14)	1.35			1.33		1.09	1.09		1.09

Product	C _a -C _b	C _a -F _a	C _a -F _b	C _b -F _a	C _b -F _b	C _a -H _a	C _a -H _b	C _b -H _a	C _b -H _b
1,1-difluoroethylene radical (2)	1.31	1.34	1.33					1.08	
<i>trans</i> -1,2-difluoroethylene radical (12)	1.33	1.36			1.31	1.08			
<i>cis</i> -1,2-difluoroethylene radical (13)	1.33	1.34			1.32	1.09			
<i>cis</i> -monofluoroethylene radical (15)	1.31	1.34				1.10			1.08
<i>trans</i> -monofluoroethylene radical (16)	1.31	1.35				1.10			1.08
monofluoroethylene radical (7)	1.32			1.32		1.09	1.08		

Product	C _a -F _a	C _a -F _b	C _a -H _a	C _a -H _b	C _a -H _c
CF ₂ (3)	1.32	1.32			
CHF (17)	1.32		1.14		
CH ₂ (8)			1.13	1.13	
Methyl radical (3)			1.08	1.08	1.08
Monofluoromethyl radical (17)	1.34		1.08	1.08	
Difluoromethyl radical (8)	1.33	1.33	1.08		

Product	H-F	H-H
hydrogen fluoride	0.92	
hydrogen molecule		0.74

Transition state	C _a -C _b	C _a -F _a	C _a -F _b	C _b -F _a	C _b -F _b	C _a -H _a	C _a -H _b	C _a -H _c	C _b -H _a	C _b -H _b	C _b -H _c	H _a -H _b
TS H shift (0 -> 4)	1.47	1.35	1.35			1.31				1.08	1.08	
TS F shift (4 -> 9)	1.37	2.04			1.33	1.08	1.09				1.08	
TS H dissociation (0 -> 1)	1.33	1.33	1.33						2.39	1.08	1.08	
TS H dissociation (4 -> 5)	1.36	1.33	1.33			1.98				1.08	1.08	
TS H dissociation (9 -> 10)	1.35	1.34			1.34	2.13	1.09				1.09	
TS H dissociation (9 -> 11)	1.35	1.34			1.34	2.16	1.09				1.09	
TS H2 elimination (1 -> 2)	1.32			1.34	1.33		1.50	1.08				0.84
TS H2 elimination (9 -> 13)	1.33	1.33			1.34		1.42				1.09	0.89
TS H2 elimination (9 -> 12)	1.33	1.32			1.35		1.42				1.09	0.89
TS HF elimination (4 -> 7)	1.35	2.26	1.33			1.15				1.09	1.08	
TS HF elimination (9 -> 15)	1.34	2.27			1.34	1.09	1.19				1.09	
TS HF elimination (9 -> 16)	1.34	2.27			1.33	1.09	1.18				1.09	
TS H shift a (9 -> 9)	1.46	1.37			1.36	1.09	1.32				1.10	
TS H shift b (9 -> 9)	1.44	1.37			1.37	1.09				1.34	1.09	
TS rotation (0 -> 0)	1.50			1.35	1.35	1.10	1.10	1.10				
TS rotation (4 -> 4)	1.48	1.38	1.38			1.10				1.08	1.09	
TS rotation a (9 -> 9)	1.49	1.39			1.35	1.10	1.11				1.09	
TS rotation b (9 -> 9)	1.50	1.38			1.34	1.11	1.11				1.09	

A.4) Angles

Angles between selected atoms within all structures are listed in the tables below. The atom labeling refers to the images in Fig.1.

Product	F _a -C _a -F _b	F _a -C _b -F _b	C _a -C _b -F _a	C _b -C _a -F _a	C _a -C _b -H _a	C _a -C _b -H _b	C _a -C _b -H _c	C _b -C _a -H _a	C _b -C _a -H _b	C _b -C _a -H _c
1,1-difluoroethyl radical (0)		109.94°	114.92°					111.23°	109.93°	109.93°
1,1-difluoroethyl radical (4)	108.11°		110.44°		119.62°	119.62°		113.56°		
1,2-difluoroethyl radical a (9)		117.47°		112.52°			124.45°	110.13°	109.43°	
1,2-difluoroethyl radical b (9)		117.47°		112.52°			124.45§	109.43°	110.13°	

Product	F _a -C _a -F _b	C _a -C _b -F _a	C _a -C _b -F _b	C _b -C _a -F _a	C _a -C _b -H _b	C _a -C _b -H _c	C _b -C _a -H _a	C _b -C _a -H _b
1,1-difluoroethene (1)	110.04°	124.98°					119.86°	119.86°
<i>cis</i> -1,2-difluoroethene (10)			123.08°	123.08°	122.20°		122.21°	
<i>trans</i> -1,2-difluoroethene (11)			120.49°	120.49°	124.77°		124.77°	
Monofluoroethene (6, 14)		122.72°				125.33°	121.36°	119.41°

Structure	F _a -C _a -F _b	C _a -C _b -F _a	C _a -C _b -F _b	C _b -C _a -F _a	C _a -C _b -H _a	C _a -C _b -H _b	C _a -H _a -F _a	C _b -C _a -H _a	C _b -C _a -H _b
1,1-difluoroethylene radical (2)	109.85°				125.48°	140.45°			
<i>trans</i> -1,2-difluoroethylene radical (12)				131.22°	123.24°			122.01°	
<i>cis</i> -1,2-difluoroethylene radical (13)				127.67°		123.92°		121.46°	
<i>cis</i> -monofluoroethylene radical (15)					125.48°		140.45°	124.67°	
<i>trans</i> -monofluoroethylene radical (16)					123.73°		137.81°	111.78°	
monofluoroethylene radical (7)		129.82°						121.39°	119.76°

Structure	H _a -C _a -H _b	H _a -C _a -H _c	H _a -C _a -F _a	H _a -C _a -F _b	F _a -C _a -F _b
CF ₂ (3)			104.03°		
CHF (17)	101.32°				
CH ₂ (8)	98.92°				
Methyl radical (3)	120.00°	120.00°			
Monofluoromethyl radical (17)	114.28°			116.63°	
Difluoromethyl radical (8)			110.67°		115.80°

Transition state	H _a -C _a -H _b	F _a -C _a -F _b	C _a -C _b -F _a	C _a -C _b -F _b	C _b -C _a -F _a	C _b -C _a -F _b	C _a -C _b -H _a	C _a -C _b -H _b	C _a -C _b -H _c	C _b -C _a -H _a	C _b -C _a -H _b	C _b -C _a -H _c	H _a -C _a -F _a
TS H shift (0 -> 4)		111.7°	117.7°					118.4°	118.4°				120.9°
TS F shift (4 -> 9)				121.1°	73.2°				125.3°	120.7°	119.9°		
TS H dissociation (0 -> 1)		110.3°			124.8°		102.9°	119.8°	119.8°				
TS H dissociation (4 -> 5)		111.1°			123.6°			119.2°	119.2°	92.9°			
TS H dissociation (9 -> 10)				122.4°	122.1°				122.3°	98.3°	121.7°		
TS H dissociation (9 -> 11)				120.2°	119.7°				124.7°	98.3°	124.3°		
TS H2 elimination (1 -> 2)	178.6°	109.9°	125.0°								116.3°	130.3°	
TS H2 elimination (9 -> 13)	178.4°			121.1°	124.5°				124.3°		121.3°		
TS H2 elimination (9 -> 12)	179.9°			123.3°	127.7°				121.9°		118.0°		
TS HF elimination (4 -> 7)		114.1°				123.32°		121.5°	118.7°	122.9°			

TS HF elimination (9 -> 15)		122.4°	109.5°			124.5°	125.8°	116.1°		
TS HF elimination (9 -> 16)		123.1°	118.2°			124.3°	122.2°	120.8°		
TS H shift a (9 -> 9)		116.8°	122.0°			125.9°	114.4°	57.3°		
TS H shift b (9 -> 9)		122.1°	122.1°			118.0°	118.0°	57.3°		
TS rotation (0 -> 0)	109.9 °	115.5°					110.1°	111.4°	110.1°	
TS rotation (4 -> 4)	106.6 °			110.28 °	121.4°	118.8°	113.7°			
TS rotation a (9 -> 9)		115.6°	109.5°			122.0°	112.6°	109.6°		
TS rotation b (9 -> 9)		116.9°	110.9°		110.67 °	122.5°		111.1°		

A.5) Dihedral angles:

Product	C _a -C _b -F _a -F _b	H _a -C _a -C _b -F _b	H _b -C _a -C _b -F _b	H _c -C _a -C _b -F _a	H _c -C _a -C _b -F _b	H _a -C _a -C _b -H _b
1,1-difluoroethyl radical (0)	131.50°	-64.54°	175.43°		55.49°	
1,1-difluoroethyl radical (4)	121.21°		-155.16°		35.08°	84.88°
1,2-difluoroethyl radical a (9)	81.21°	-39.03°	-159.13°		-73.67°	
1,2-difluoroethyl radical b (9)	-81.21°	159.12°	39.03°	73.67°		

Product	C _a -C _b -F _a -F _b	H _a -C _a -C _b -F _a	H _a -C _a -C _b -F _b	H _b -C _a -C _b -F _a	H _b -C _a -C _b -F _b	H _c -C _a -C _b -F _a
1,1-difluoroethene (1)	180.00°		180.00°		0.00°	
<i>cis</i> -1,2-difluoroethene (10)	0.00°		180.00°	180.00°		
<i>trans</i> -1,2-difluoroethene (11)	180.00°		0.00°	0.00°		
Monofluoroethene (6, 14)		0.00°		180.00°		180.00°

Product	C _a -C _b -F _a -F _b	H _a -C _a -C _b -F _a	H _a -C _a -C _b -F _b	H _b -C _a -C _b -F _a	H _b -C _a -C _b -F _b
CF ₂ (3)	180.00°		180.00°		
CHF (17)	0.00°	180.00°			
CH ₂ (8)	180.00°		0.00°		
Methyl radical (3)		180.00°		0.00°	
Monofluoromethyl radical (17)		180.00°		180°	
Difluoromethyl radical (8)		0.00°			180.00°

Structure	H _a -C _a -H _b -H _c	H _a -C _a -F _a -H _b	H _a -C _a -F _b -F _b
Methyl radical (3)	180.00°		
Monofluoromethyl radical (17)		-140.93°	
Difluoromethyl radical (8)			-144.41°

Transition state	C _a -C _b -F _a -F _b	H _a -C _a -C _b -F _a	H _a -C _a -C _b -F _b	H _b -C _a -C _b -F _a	H _b -C _a -C _b -F _b	H _c -C _a -C _b -F _a	H _c -C _a -C _b -F _b	C _a -F _a -F _b -H _a	H _a -C _a -C _b -H _b	H _c -C _a -C _b -H _c
------------------	----------------------------------------------------------------	----------------------------------------------------------------	----------------------------------------------------------------	----------------------------------------------------------------	----------------------------------------------------------------	----------------------------------------------------------------	----------------------------------------------------------------	----------------------------------------------------------------	----------------------------------------------------------------	----------------------------------------------------------------

TS H shift (0 -> 4)	140.71°			-151.08°	12.72°	151.69°
TS F shift (4 -> 9)	97.17°	1.44°		-173.65°	-86.53°	
TS H dissociation (0 -> 1)	-178.88°	89.36°		-178.09°	-3.19°	
TS H dissociation (4 -> 5)	165.64°			-175.42°	11.55°	86.51°
TS H dissociation (9 -> 10)	6.86°	-100.25°		174.43°	-177.85°	
TS H dissociation (9 -> 11)	176.93°	-76.97°		8.27°	-6.43°	
TS H2 elimination (1 -> 2)	-180.00°			0.00°	-180.00°	179.99°
TS H2 elimination (9 -> 13)	180.00°			0.00°	0.00°	-180.00°
TS H2 elimination (9 -> 12)	0.00°			180.00°	180.00°	180.00°
TS HF elimination (4 -> 7)	146.68°			-10.97°	173.80°	169.30°
TS HF elimination (9 -> 15)	-164.89°	-15.405°		170.57°	18.37°	
TS HF elimination (9 -> 16)	23.19°	169.81°		-5.35°	-161.83°	
TS H shift a (9 -> 9)	-37.95°	178.60°		89.62°	116.09°	
TS H shift b (9 -> 9)	-114.68°	34.11°	122.66°		34.11°	
TS rotation (0 -> 0)	132.82°	-125.28°		114.93°	-4.86°	
TS rotation (4 -> 4)	119.69°		-121.30°		58.71°	-180.00°
TS rotation a (9 -> 9)	-150.91°	89.08°		-30.31°	-2.49°	
TS rotation b (9 -> 9)	0.27°	-120.98°		120.84°	151.42°	

B) Absolute Energies

Table 1: Absolute Energies of Products derived at the HCTH147/6-31G** and the CCSD(T)/cc-pVTZ levels of theory

Product	HCTH147/6-31G**	CCSD(T)/cc-pVTZ
1, 1-difluoroethyl radical (0)	-277.5539	-277.2333
1, 1 -difluoroethene (1, 5)	-276.9846	-276.6726
1, 1 -difluoroethenyl radical (2)	-276.2975	-275.9889
methyl radical (3)	-39.8169	-39.7315
CF ₂ (3)	-237.6419	-237.4118
1, 1-difluoroethyl radical (4)	-277.5432	-277.2286
monofluoroethene (6, 14)	-177.7615	-177.5278
monofluoroethenyl radical (7)	-177.0854	-176.8527
difluoromethyl radical (8)	-238.2496	-238.0056
CH ₂ (8)	-39.1126	-39.0451
1, 2-difluoroethyl radical (9, rotamer a)	-277.5318	-277.2145
1, 2-difluoroethyl radical (9, rotamer b)	-277.5318	-277.2145
<i>cis</i> -1, 2-difluoroethene (10)	-276.9665	-276.6562
<i>trans</i> -1, 2-difluoroethene (11)	-276.9664	-276.6556
<i>cis</i> -1, 2-difluoroethenyl (12)	-276.2860	-275.9758
<i>trans</i> - 1, 2 -difluoroethenyl radical (13)	-276.2858	-275.9757
<i>cis</i> -monofluoroethenyl radical (15)	-177.0777	-176.8472
<i>trans</i> -monofluoroethenyl radical (16)	-177.0778	-176.8485
monofluoromethyl radical (17)	-139.0253	-138.8616
CFH (17)	-138.3676	-138.2165
hydrogenfluoride (7, 15, 16)	-100.4053	-100.3291
hydrogen molecule (1, 5, 10, 11)	-1.1781	-1.1623
fluorine atom (6, 14)	-99.6896	-99.6204
hydrogen atom (1, 5, 10, 11)	-0.5065	-0.4998

Table 2: Absolute Energies of Transition States derived at the HCTH147/6-31G** and the CCSD(T)/cc-pVTZ levels of theory

Transition state	HCTH147/6-31G**	CCSD(T)/cc-pVTZ
TS H dissociation (0 -> 1)	-277.4865	-277.1698
TS H shift(0 -> 4)	-277.4783	-277.1528
TS H ₂ elimination (1 -> 2)	-277.4699	-277.1395
TS H dissociation (4 -> 5)	-277.4798	-277.1619
TS HF elimination (4 -> 7)	-277.4790	-277.1434
TS F shift(4 -> 9)	-277.4940	-277.1641
TS H dissociation (9 -> 10)	-277.4658	-277.1491
TS H dissociation (9 -> 11)	-277.4657	-277.1491
TS HF elimination (9 -> 15)	-277.4771	-277.1432
TS HF elimination (9 -> 16)	-277.4759	-277.1421
TS H ₂ elimination (10 -> 12)	-277.4543	-277.1233
TS H ₂ elimination (10 -> 13)	-277.4551	-277.1244
TS rotation (0 -> 0)	-277.5507	-277.2304
TS rotation (4 -> 4)	-277.5427	-277.2275
TS H-shift a (9 -> 9)	-277.4663	-277.1394
TS H-shift b (9 -> 9)	-277.4576	-277.1321
TS rotation a (9 -> 9)	-277.5279	-277.2115
TS rotation b (9 -> 9)	-277.5236	-277.2066

C) Zero-point Energy (ZPE)

Table 3: Zero-point Energies of products derived by frequency analysis using the HCTH147/6-31G** level of theory.

Product	ZPE [HF]
1, 1-difluoroethyl radical (0)	0.0462
1, 1 -difluoroethene (1, 5)	0.0361
1, 1 -difluoroethenyl radical (2)	0.0227
methyl radical (3)	0.0294
CF ₂ (3)	0.0067
1, 1-difluoroethyl radical (4)	0.0455
monofluoroethene (6, 14)	0.0430
monofluoroethenyl radical (7)	0.0300
difluoromethyl radical (8)	0.0186
CH ₂ (8)	0.0157
1, 2-difluoroethyl radical (9, rotamer a)	0.0455
1, 2-difluoroethyl radical (9, rotamer b)	0.0455
<i>cis</i> -1, 2-difluoroethene (10)	0.0360
<i>trans</i> -1, 2-difluoroethene (11)	0.0358
<i>cis</i> -1, 2-difluoroethenyl radical (12)	0.0236
<i>trans</i> - 1, 2 -difluoroethenyl radical (13)	0.0232
<i>cis</i> -monofluoroethenyl radical (15)	0.0297
<i>trans</i> -monofluoroethenyl radical (16)	0.0294
monofluoromethyl radical (17)	0.0240
CFH (17)	0.0118
hydrogenfluoride (7, 15, 16)	0.0092
hydrogen molecule (1, 5, 10, 11)	0.0101

Table 4: Zero-point Energies of transition states derived by frequency analysis using the HCTH147/6-31G** level of theory.

Transition state	ZPE [HF]
TS (0 -> 1)	0.0366
TS (0 -> 4)	0.0400
TS (1 -> 2)	0.0340
TS (4 -> 5)	0.0371
TS (4 -> 7)	0.0411
TS (4 -> 9)	0.0439
TS (9 -> 10)	0.0373
TS (9 -> 11)	0.0370
TS (9 -> 15)	0.0414
TS (9 -> 16)	0.0413
TS (10 -> 12)	0.0354
TS (10 -> 13)	0.0351
TS rotation (0 -> 0)	0.0455
TS rotation (4 -> 4)	0.0446
TS H-shift a (9 -> 9)	0.0412
TS H-shift b (9 -> 9)	0.0408
TS rotation (9 -> 9)	0.0443
TS rotation (9 -> 9)	0.0445

D) CCSD(T) optimized geometries and resulting energies

Table 5: DFT-optimized structures CCSD(T)/cc-pVTZ single point energies relative to the 1,1-difluoroethyl radical compared to CCSD(T) optimized structures. Energies are in kcal/mol and not corrected by zero-point energies.

Product/ transition state	DFT-optimized [kcal/mol]	CC-optimized [kcal/mol]	Difference [kcal/mol]
1,1-difluoroethyl radical (0)	0.0000	0.0000	0.0000
1,1-difluoroethene (1)	44.4775	44.5844	0.1068
1,1-difluoroethylene radical (2)	59.9022	59.9641	0.0619
methyl radical & CF ₂ (3)	62.7805	62.5670	-0.2135
TS rotation (0 -> 0)	2.2317	2.2573	0.0255
TS H ₂ elimination (1 -> 2)	21.9904	21.9132	-0.0773

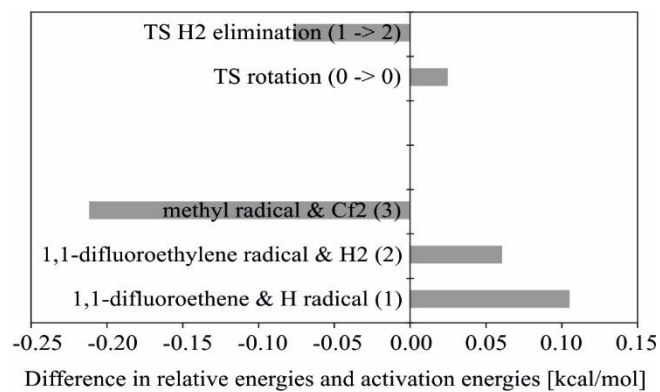


FIG 1: Energy differences between DFT optimized structures CCSD(T)/cc-pVTZ single point energies and CC optimized structures relative to the 1,1-difluoroethyl radical in kcal/mol.

E) Excited States

E.1) Vertical Excitations

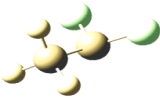
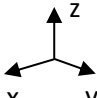
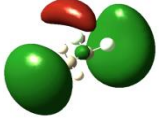

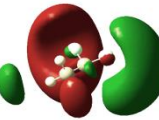
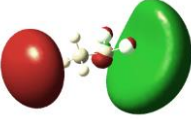
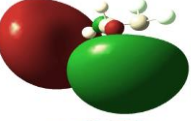
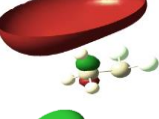

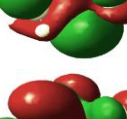
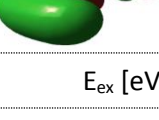
1, 1-difluoroethyl radical (0)									
		Ground State	1. excited State	2. excited State	3. excited State	4. excited State	5. excited State	6. excited State	7. excited State
	22 (3d _{z2})	—	—	—	—	—	—	—	↑
	21b (3d _{xz})	—	—	—	—	—	—	↑	—
	23α (3d _{xy})	—	—	—	—	—	↑	—	—
	21α (3p _x)	—	—	—	—	↑	—	—	—
	19α (3p _y)	—	—	—	↑	—	—	—	—
	20α (3p _z)	—	—	↑	—	—	—	—	—
	18α (3s)	—	↑	—	—	—	—	—	—
	17α (σ)	↑	—	—	—	—	—	↑	—
	16 (σ)	↑↓	↑↓	↑↓	↑↓	↑↓	↑↓	↑	↑↓
E_{ex} [eV]		0	6.06	6.92	7.14	7.17	7.56	7.80	7.98
f_{osc}			0.001	0.061	0.009	0.016	0.006	0.006	0.004

FIG 2: Electronic configurations of the ground state and the first seven excited states of S1. Excitations mainly take place from the σ -type SOMO to higher lying orbitals, which are Rydberg states at most. Shown are only orbital pictures which have main contributions to the actually mixed excited state. To excited state number four, also the $3p_z$ Rydberg state in addition to the $3p_x$ state has a large MO-coefficient. Excitation energies in electron volts as well as oscillator strength are given beyond the corresponding electronic configuration. The orbital numbering is arbitrarily chosen and characterization of orbitals is given wherever possible.


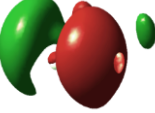
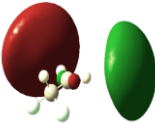
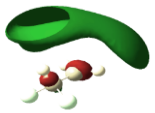
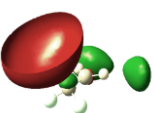


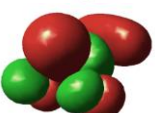

Orbital type		Ground State	1. excited State	2. excited State	3. excited State	4. excited State	5. excited State	6. excited State	7. excited State
	22α	—	—	—	—	—	—	—	↑
	21α (3d _{xy})	—	—	—	—	—	—	↑	—
	20α (3p _z)	—	—	—	—	—	↑	—	—
	19α (3s)	—	—	—	—	↑	—	—	—
	18α	—	—	↑	—	—	—	—	—
	20b (π)	—	↓	—	↓	—	—	—	—
	17α (π)	↑	↑	—	↑	—	—	—	—
	16 (σ)	↑↓	↑	↑↓	↑↓	↑↓	↑↓	↑↓	↑↓
	15 (σ)	↑↓	↑↓	↑↓	↑	↑↓	↑↓	↑↓	↑↓
E_{ex} [eV]		0	6.02	6.44	6.89	7.23	7.50	8.04	8.16
f_{osc}			0.001	0.025	0	0.021	0	0.002	0.005

FIG 3: Electronic configurations of the ground state and the first seven excited states of S2. Excitations mainly take place from the σ -type SOMO to higher lying orbitals, which are Rydberg states at most. Shown are only orbital pictures which have main contributions to the actually mixed excited state. Excitation energies in electron volts as well as oscillator strength are given beyond the corresponding electronic configuration. The orbital numbering is arbitrarily chosen and characterization of orbitals is given wherever possible.

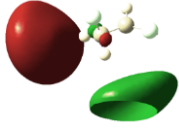
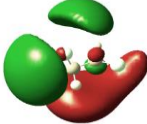

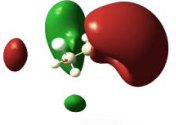

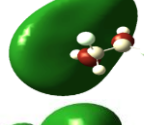
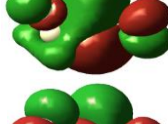
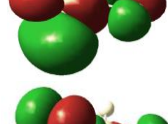
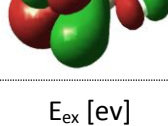
Orbital type		Ground State	1. Excited State	2. Excited State	3. Excited State	4. Excited State	5. Excited State	6. Excited State	7. Excited State
	20α (3p _y)	—	—	—	—	—	—	—	↑
	21α (3d _{xz})	—	—	—	—	—	—	↑	—
	19α	—	—	—	—	↑	—	—	—
	22α (3d _{xy})	—	—	—	↑	—	—	—	—
	20b (π)	—	—	↓	—	—	↓	—	—
	18α (3s)	—	↑	—	—	—	—	—	—
	17α	↑	—	↑	—	—	↑	—	—
	16 (σ)	↑↓	↑↓	↑	↑↓	↑↓	↑↓	↑↓	↑↓
	15 (σ)	↑↓	↑↓	↑↓	↑↓	↑↓	↑	↑↓	↑↓
E_{ex} [ev]		0	5.98	6.03	6.56	6.75	7.04	7.37	7.52
f_{osc}			0.016	0.005	0.002	0.004	0	0.019	0

FIG 4: Electronic configurations of the ground state and the first seven excited states of S3a. Excitations mainly take place from the σ -type SOMO to higher lying orbitals, which are Rydberg states at most. Shown are only orbital pictures which have main contributions to the actually mixed excited state. Excitation energies in electron volts as well as oscillator strength are given beyond the corresponding electronic configuration. The orbital numbering is arbitrarily chosen and characterization of orbitals is given wherever possible.

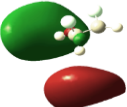
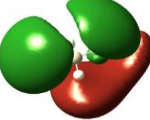
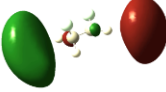
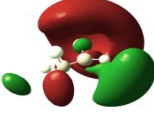




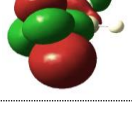
Orbital type		Ground State	1. Excited State	2. Excited State	3. Excited State	4. Excited State	5. Excited State	6. Excited State	7. Excited State
	20a (3p _y)	—	—	—	—	—	—	—	↑
	21a (3d _{xz})	—	—	—	—	—	—	↑	—
	19a (3p _x)	—	—	—	—	↑	—	—	—
	22a (3d _{xy})	—	—	—	↑	—	—	—	—
	20b	—	—	↓	—	—	↓	—	—
	18a (3s)	—	↑	—	—	—	—	—	—
	17a	↑	—	↑	—	—	↑	—	—
	16 (σ)	↑↓	↑↓	↑	↑↓	↑↓	↑↓	↑↓	↑↓
	15 (σ)	↑↓	↑↓	↑↓	↑↓	↑↓	↑	↑↓	↑↓
E _{ex} [ev]		0	5.98	6.03	6.56	6.75	7.04	7.37	7.52
f _{osc}			0.016	0.005	0.002	0.004	0	0.019	0

FIG 5: Electronic configurations of the ground state and the first seven excited states of S1. Excitations mainly take place from the σ -type SOMO to higher lying orbitals, which are Rydberg states at most. Shown are only orbital pictures which have main contributions to the actually mixed excited state. Excitation energies in electron volts as well as oscillator strength are given beyond the corresponding electronic configuration. The orbital numbering is arbitrarily chosen and characterization of orbitals is given wherever possible.

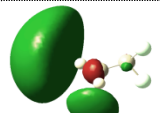
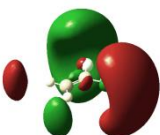
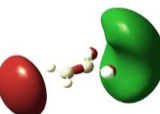





Orbital type		Ground State	1. excited State	2. excited State	3. excited State	4. excited State	5. excited State	6. excited State	7. excited State
	18 <i>t</i>	—	—	—	—	—	—	—	↑
	22α (3d _{xy})	—	—	—	—	—	—	↑	—
	19α (3p _x)	—	—	—	—	—	↑	—	—
	18α (3p _y)	—	—	—	—	↑	—	—	—
	20α (3p _z)	—	—	—	↑	—	—	—	—
	17α (??)	—	—	↑	—	—	—	—	—
	17 <i>t</i>	—	↑	—	—	—	—	—	—
	16 (π)	↑↓	↑	↓	↓	↓	↓	↓	↑
E_{ex} [eV]		0	2.64	7.11	7.90	8.17	8.24	8.79	8.97
f_{osc}			0	0.047	0.274	0	0	0	0

FIG 6 Electronic configurations of the ground state and the first seven excited states of S1. Excitations mainly take place from the σ -type SOMO to higher lying orbitals, which are Rydberg states at most. Shown are only orbital pictures which have main contributions to the actually mixed excited state. Excitation energies in electron volts as well as oscillator strength are given beyond the corresponding electronic configuration. The orbital numbering is arbitrarily chosen and characterization of orbitals is given wherever possible. A *t* indicates that the configuration corresponds to a triplet state.

E.2) Non-adiabatic excitations:

Table 6: nonadiabatic excitation energies derived by structure optimization with EOMEE-CCSD/aug-cc-pVDZ

Product	Excitation energy [eV]
1, 1-difluoroethyl radical (0)	4.11
1, 1-difluoroethene (1)	2.61
1, 1-difluoroethyl radical (4)	4.01
1, 2-difluoroethyl radical (9, rotamer a)	5.56
1, 2-difluoroethyl radical (9, rotamer b)	5.56

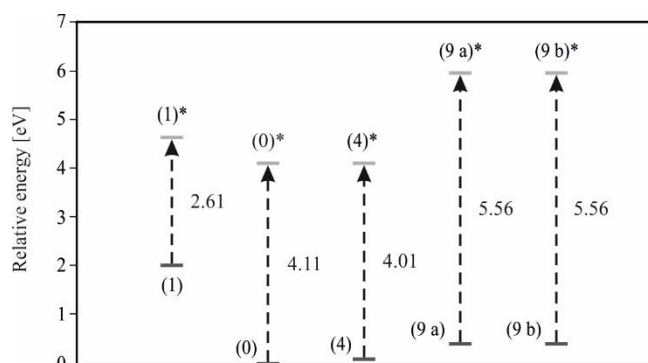


FIG 7: nonadiabatic excitation energy scheme

Geometries optimized in the first electronically excited state resemble much the ones of cationic structures. The following tables contain Cartesian coordinates of cationic and excited state structures.

1, 1-difluoroethyl radical (0) cationic structure			
Atom	Coordinates [Å]		
	x	y	z
C	-0.003154	-1.393687	0.000000
C	-0.013344	0.052734	0.000000
F	-0.003154	0.740191	1.061538
F	-0.003154	0.740191	-1.061538
H	1.063134	-1.702654	0.000000
H	-0.453692	-1.787535	0.917264
H	-0.453692	-1.787535	-0.917264

1, 1-difluoroethyl radical (0) excited state structure			
Atom	Coordinates [Å]		
	x	y	z
C	1.506344	0.000055	0.008194
C	0.046750	0.000005	0.002811
F	-0.635726	-1.073292	0.000585
F	-0.635812	1.073247	0.000585
H	1.733455	-0.000143	-1.098420
H	1.871869	0.932755	0.472509
H	1.871897	-0.932487	0.472825

1, 1-difluoroethyl radical (4) excited state structure			
Atom	Coordinates [Å]		
	x	y	z
C	0.046750	-0.000005	0.002811
C	1.506344	-0.000054	0.008194
F	-0.635727	1.073291	0.000585
F	-0.635812	-1.073248	0.000585
H	1.871896	0.932488	0.472824
H	1.871869	-0.932754	0.472824
H	1.733455	0.000143	-1.098420

1, 2-difluoroethyl radical (9 a) cationic structure			
-----------------------------------------------------	--	--	--

Atom	Coordinates [Å]		
	x	y	z
C	-0.737773	-0.782314	0.162880
C	0.453099	-0.204932	-0.487253
F	1.438124	0.168711	0.212444
F	-1.178853	0.585216	0.033612
H	-0.636818	-1.054713	1.216196
H	0.499151	0.045752	-1.553422
H	-1.360263	-1.448269	-0.438892

1, 2-difluoroethyl radical (9 b) cationic structure			
Atom	Coordinates [Å]		
	x	y	z
C	-0.737773	-0.782313	-0.162880
C	0.453099	-0.204932	0.487253
F	-1.178852	0.585216	-0.033612
F	1.438124	0.168710	-0.212444
H	-1.360264	-1.448268	0.438892
H	0.499151	0.045752	1.553422
H	-0.636819	-1.054712	-1.216196

1, 1-difluoroethene radical (1) triplet state structure			
Atom	Coordinates [Å]		
	x	y	z
C	-0.375760	-0.269862	0.280609
C	0.818238	0.542735	0.065050
F	-0.297398	-1.548265	-0.153187
F	-1.536258	0.272062	-0.153204
H	1.386148	0.929225	0.906131
H	1.161020	0.776017	-0.945380

F) Augmented basis set calculations

Structures containing fluorine atoms should be treated in calculations with additional polarization functions in the basis set. We do calculations with augmented basis sets and compare the results with the ones of non-augmented basis set calculations.

Table 7: Comparison between relative energies of products based on HCTH147/6-31G** and the augmented basis set method HCTH147/6-31++G** with 1,1-difluoroethyl radical as reference.

Product	Relative energy [kcal/mol]	
	HCTH147/6-31G**	HCTH147/6-31++G**
(0)	0	0
(4)	6.67	5.08
(9 a)	13.81	10.59
(9b)	13.81	10.59
(1)	39.38	39.73
(5)	39.38	39.73
(10)	50.75	48.65
(11)	50.77	49.29
(2)	49.08	49.74
(12)	56.29	56.04
(13)	56.42	56.85
(6)	64.50	59.85
(14)	64.50	59.85
(7)	39.62	30.26
(15)	44.44	34.68
(16)	44.40	34.03
(3)	59.58	58.16
(8)	120.16	119.68
(17)	100.94	98.93

Table 8: Comparison between relative energies of transition states based on HCTH147/6-31G** and the augmented basis set method HCTH147/6-31++G** with 1,1-difluoroethyl radical as reference.

Product	Relative energy [kcal/mol]	
	HCTH147/6-31G**	HCTH147/6-31++G**
TS (0 -> 4)	47.39	46.10
TS (4 -> 9 a)	37.55	30.38
TS (0 -> 1)	42.23	43.17

TS (4 -> 5)	46.46	47.28
TS (9 -> 10)	55.23	47.39
TS (9 -> 11)	55.31	56.74
TS (1 -> 2)	52.64	53.76
TS (10 -> 12)	61.93	61.21
TS (10 -> 13)	62.41	62.40
TS (4 -> 7)	46.92	41.60
TS (9 -> 15)	48.11	42.19
TS (9 -> 16)	48.87	43.29
TS H-shift a (9 -> 9)	60.35	52.00
TS H-shift b (9 -> 9)	54.89	57.45
TS rotation (0 -> 0)	1.96	1.68
TS rotation (4 -> 4)	7.03	5.11
TS rotation (9 -> 9)	16.28	13.59
TS rotation (9 -> 9)	18.99	16.91

Table 9: Comparison between relative energies of products based on CCSD(T)/cc-pVTZ and the augmented basis set method CCSD(T)/aug-cc-pVTZ with 1,1-difluoroethyl radical as reference.

Product	Relative energy [kcal/mol]	
	CCSD(T)/cc-pVTZ	CCSD(T)/aug-cc-pVTZ
(0)	0	0
(4)	2.91	2.78
(9 a)	11.74	11.06
(9b)	11.74	11.06
(1)	38.16	39.51
(5)	38.16	39.51
(10)	48.45	47.02
(11)	48.80	49.57
(2)	51.43	52.66
(12)	59.67	60.61
(13)	59.71	61.16
(6)	53.40	54.94
(14)	53.40	54.94
(7)	32.30	31.95
(15)	35.74	35.08
(16)	34.96	34.13
(3)	56.43	57.72
(8)	114.43	114.69
(17)	97.35	97.75

Table 10: Comparison between relative energies of transition states based on CCSD(T)/cc-pVTZ and the augmented basis set method CCSD(T)/aug-cc-pVTZ with 1,1-difluoroethyl radical as reference.

Product	Relative energy [kcal/mol]	
	CCSD(T)/cc-pVTZ	CCSD(T)/aug-cc-pVTZ
(0 -> 4)	50.45	50.11
(4 -> 9 a)	43.34	40.42
TS (0 -> 1)	39.98	40.73
TS (4 -> 5)	44.74	45.40
TS (9 -> 10)	52.77	45.51
TS (9 -> 11)	52.81	56.59
TS (1 -> 2)	58.77	59.74
TS (10 -> 12)	68.29	68.41
TS (10 -> 13)	68.96	69.57
TS (4 -> 7)	56.33	55.96
TS (9 -> 15)	56.48	55.76
TS (9 -> 16)	57.16	56.56
TS H-shift a (9 -> 9)	63.41	57.99
TS H-shift b (9 -> 9)	58.89	62.60
TS rotation (0 -> 0)	1.78	1.79
TS rotation (4 -> 4)	3.62	3.35
TS rotation (9 -> 9)	13.67	13.15
TS rotation (9 -> 9)	16.70	16.21

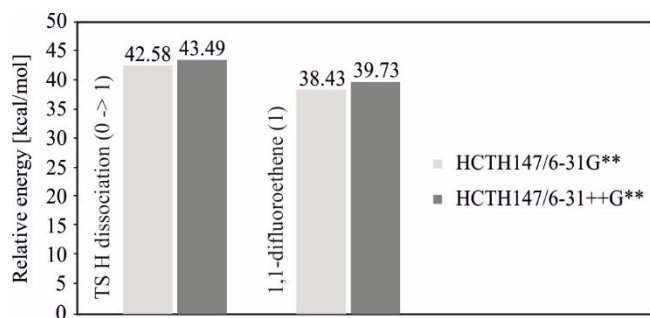


FIG 8: Comparison of energies of transition state and product of the H dissociation reaction channel outgoing from 1,1-difluoroethyl radical relative to the 1,1-difluoroethyl radical energy based on the HCTH/6-31G** to augmented basis set HCTH/6-31++G**.

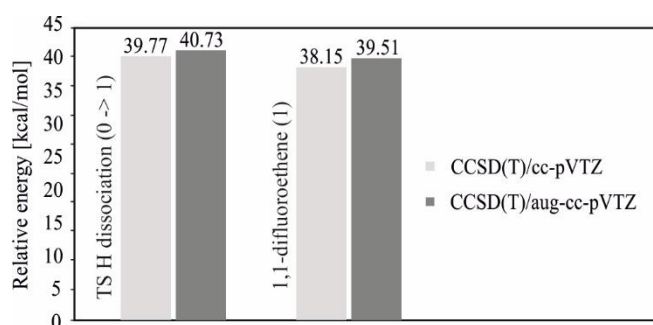


FIG 9: Comparison of energies of transition state and product of the H dissociation reaction channel outgoing from 1,1-difluoroethyl radical relative to the 1,1-difluoroethyl radical energy based on the HCTH/6-31G** to augmented basis set HCTH/6-31++G**.

G) CCSD(T)/ cc-pVTZ-F12 calculations

Table 11: Comparison between relative energies of products based on CCSD(T)/cc-pVTZ and CCSD(T)/ cc-pVTZ-F12 with 1,1-difluoroethyl radical as reference.

Product	Relative energy [kcal/mol] CCSD(T)/cc-pVTZ	Relative energy [kcal/mol] CCSD(T)/cc-pVTZ-F12
(0)	0	0
(1)	38.2	38.9
(3)	56.4	58.2
(4)	2.9	2.9

Table 12: Comparison between relative energies of transition states based on CCSD(T)/cc-pVTZ and CCSD(T)/ cc-pVTZ-F12 with 1,1-difluoroethyl radical as reference.

Product	Relative energy [kcal/mol] CCSD(T)/cc-pVTZ	Relative energy [kcal/mol] CCSD(T)/cc-pVTZ-F12
TS (0 → 1)	39.8	40.0
TS (0 → 4)	50.4	49.8